A Journey Through a Leaf: Phenomics Analysis of Leaf Growth in Arabidopsis thaliana

Authors: Vanhaeren, Hannes, Gonzalez, Nathalie, and Inzé, Dirk

Source: The Arabidopsis Book, 2015(13)

Published By: The American Society of Plant Biologists

URL: https://doi.org/10.1199/tab.0181

First published on July 22, 2015: e0181. doi: 10.1199/tab.0181

A Journey Through a Leaf: Phenomics Analysis of Leaf Growth in *Arabidopsis thaliana*

Hannes Vanhaeren[a,b], Nathalie Gonzalez[a,b], Dirk Inzé[a,b,1]

[a]Department of Plant Systems Biology, VIB, B-9052 Gent, Belgium
[b]Department of Plant Biotechnology and Bioinformatics, Ghent University, B-9052 Gent, Belgium
[1]Address correspondence to dirk.inze@psb.vib-ugent.be

In Arabidopsis, leaves contribute to the largest part of the aboveground biomass. In these organs, light is captured and converted into chemical energy, which plants use to grow and complete their life cycle. Leaves emerge as a small pool of cells at the vegetative shoot apical meristem and develop into planar, complex organs through different interconnected cellular events. Over the last decade, numerous phenotyping techniques have been developed to visualize and quantify leaf size and growth, leading to the identification of numerous genes that contribute to the final size of leaves. In this review, we will start at the Arabidopsis rosette level and gradually zoom in from a macroscopic view on leaf growth to a microscopic and molecular view. Along this journey, we describe different techniques that have been key to identify important events during leaf development and discuss approaches that will further help unraveling the complex cellular and molecular mechanisms that underlie leaf growth.

INTRODUCTION

Different plants species produce leaves that are very diverse in size and shape, ranging for example from the huge leaves of giant rhubarb to the small leaves of *Arabidopsis thaliana*. Between accessions of a species and even within a single plant, leaf characteristics can differ significantly (Kerstetter and Poethig, 1998; Pérez-Pérez et al., 2002). Such observable traits are commonly referred to as phenotypes, making phenomics the biological research area that focuses on describing and measuring these phenotypes. Many traits, such as leaf growth, are not only determined by multiple genetic factors, but also by a plethora of environmental factors, such as water and nutrient availability, light, day length (Cookson et al., 2007), and by the interaction between both (El-Soda et al., 2014). Generally, phenotypes are scored as a deviation from a control, for example a wild-type (WT) background or an environmental control condition, therefore all other parameters need to be kept constant to make the correct conclusions. Since the final plant phenotype can be influenced by micro-environmental fluctuations in growth chambers of different research groups (Massonnet et al., 2010) and even by the position within a growth room, solid experimental setups (Poorter et al., 2012) and if possible, randomization of plants across the growth room are indispensable.

Phenotypes can be observed on the macroscopic, microscopic and molecular level. New techniques are constantly being developed to facilitate and improve quantitative plant phenomics, bringing us from destructive to non-destructive and even high-throughput phenotyping. Three important aspects of phenotyping that are continuously subjected to improvement are the resolution (spatial and temporal), the throughput (how many samples can be analyzed in a given time) and the dimensionality (which phenotypic traits can be measured and how many conditions and genotypes can be screened) (Dhondt et al., 2013), but simultaneously improving these three aspects remains very challenging. This chapter will mainly focus on phenomics of the Arabidopsis rosette and leaf, although many techniques presented here can also be applied to other organs, such as flower petals. For the described methods, advantages and possible drawbacks will be highlighted.

By gradually increasing the resolution of an observed phenotype, answers to the questions “What?” (What is changed in terms of growth), “Where?” (Where/in which leaves is the phenotype observed?), “When?” (When during development are the changes occurring and which are the cellular processes that are affected?) and “Why?” (Why do changes in molecular mechanisms drive these phenotypic changes?) can be found (Figure 1), extending our knowledge of the genetic networks controlling leaf size. Considering plant phenotypes at these different levels can increase our understanding of the relation between the environment, genotype and the resulting phenotype (Granier and Vile, 2014).

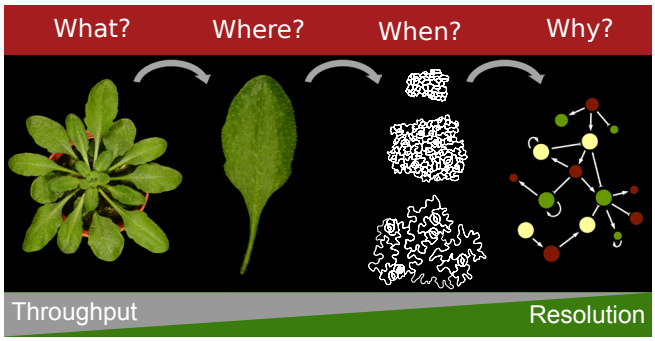

Figure 1. Throughput and resolution in leaf phenomics.

The gradual increase in phenotyping resolution from the rosette to the leaf, the leaf to the cells and cells to genes, helps answering scientific questions in plant research at different levels. Generally, a higher resolution of phenotyping comes at a cost of lower throughput.

THE ARABIDOPSIS ROSETTE

In contrast to animals, plants continuously produce new organs at meristematic tissues, such as leaves, and can also form adventitious organs, such as lateral roots, throughout their life span. During the vegetative developmental phase of *Arabidopsis thaliana*, leaves arise from the shoot apical meristem (SAM) as rod-shaped structures in a spiral pattern with very short internodes between them. Throughout their development, leaves undergo different growth stages to mature into planar, photosynthetic organs organized in a flat rosette with little overlap (Figure 1) (Rodriguez et al., 2014). When transitioning to the reproductive, flowering stage, the vegetative SAM transforms into an inflorescence meristem that gives rise to cauline leaves and flowers (Alvarez-Buylla et al., 2010; Chandler, 2012). The small size of Arabidopsis and its short life span facilitate numerous quantitative phenotyping methods. The most basic way to quantify rosette size is to measure fresh and dry weights of the plants at the end of the vegetative stage, giving insight in the plant's areal biomass. This method is however destructive and does not allow following the same individual over time to increase the resolution of the measurements. For this reason, non-destructive imaging of plants has been a widely used solution (Figure 2a).

Non-destructive rosette imaging in the visible spectrum

The primary advantage of imaging the entire rosette is that it allows high-throughput screening. Pictures can be taken at a single timepoint to measure plant size (Figure 2a) or over time to measure rosette growth (Figure 2b) (Leister et al., 1999; Zhang et al., 2012). Over the last years, several specialized automated growth platforms equipped with imaging systems have been developed (Granier et al., 2006; Walter et al., 2007; Jansen et al., 2009; Arvidsson et al., 2011; Skirycz et al., 2011b; Tisné et al., 2013; Apelt et al., 2015). These setups are often combined with specialized image analysis methods to obtain rosette growth measurements. Some platforms allow weighing and irrigating each pot according to a predetermined watering regime, facilitating flexible and reproducible drought treatments (Granier et al., 2006; Skirycz et al., 2011b; Tisné et al., 2013). Such automated phenotyping platforms are generally built in dedicated growth cabinets or chambers which are monitored to keep environmental conditions as stable as possible. To correct for micro-environmental gradients throughout the growth room, some platforms allow for the randomization of plants (Tisné et al., 2013). Generally, plants are grown in separate soil-filled pots, however systems exist in which plants grow hydroponically (Harbinson et al., 2012). On a daily basis, a top-view picture is taken from the growing rosette (Figure 2a) which can be separated from the background, such as the pot and soil. The rosette is isolated from the original images through image segmentation. This can be based on splitting the images in their red, blue and green (RGB) channels (Figure 2a) (Leister et al., 1999) or by the non-linear conversion of RGB: the hue, saturation and value (HSV) color space (Walter et al., 2007), for which the hue is the most important dimension to discriminate plants from a background (De Vylder et al., 2012). Alternatively, in case of gray-scale images, watershed-based segmentation can be performed (Apelt et al., 2015). The isolated rosette can then be converted into a binary image (Figure 2a), enabling a variety of measurements (Box 1). First of all, the projected rosette area can be measured, revealing effects of environmental or genotype specific deviations in growth compared to control situations. Other rosette characteristics, such as the perimeter and its convex hull (Figure 2a) are used to calculate parameters such as the surface coverage and stockiness of the rosette (Box 1). Surface coverage is the ratio between the projected rosette area and the convex hull and describes how much of the surface of the convex hull is occupied by the rosette. Plants composed of numerous leaves with short petioles will have a high surface coverage. The stockiness is a mathematical measure of the roundness of the rosette. If a rosette shows strong indentations, for example caused by elongated petioles or leaves, the stockiness is low (Jansen et al., 2009) (Box 1). Over the past years, the use of automated growth platforms has allowed large-scale experiments that are challenging to carry out manually. For example, by screening a collection of Arabidopsis transgenic lines showing an increased tolerance to lethal stress, it was found that these genotypes do not show an enhanced tolerance to mild drought stress conditions (Skirycz et al., 2011b). In addition, by quantifying various shoot growth parameters for a recombinant inbred line (RIL) population, quantitative trait loci (QTLs) that control plant rosette growth have been identified (Tisné et al., 2013).

A similar, fully automated phenotyping system has also been developed to measure *in vitro*-grown plants over time (Dhondt et al., 2014). In such a setup, petri dishes are positioned on a rotating disk and presented on an hourly basis to a mounted camera. With this high temporal resolution of imaging, additional observations can be made, such as diurnal movements of the rosette leaves. These changes of the leaf elevation angle, known as hyponasty, are influenced by temperature (Vile et al., 2012), circadian rhythm and light conditions (Dornbusch et al., 2014), and can be measured using laser scanning techniques (Dornbusch et al., 2012) or by combining focused and depth images of the rosette (Apelt et al., 2015).

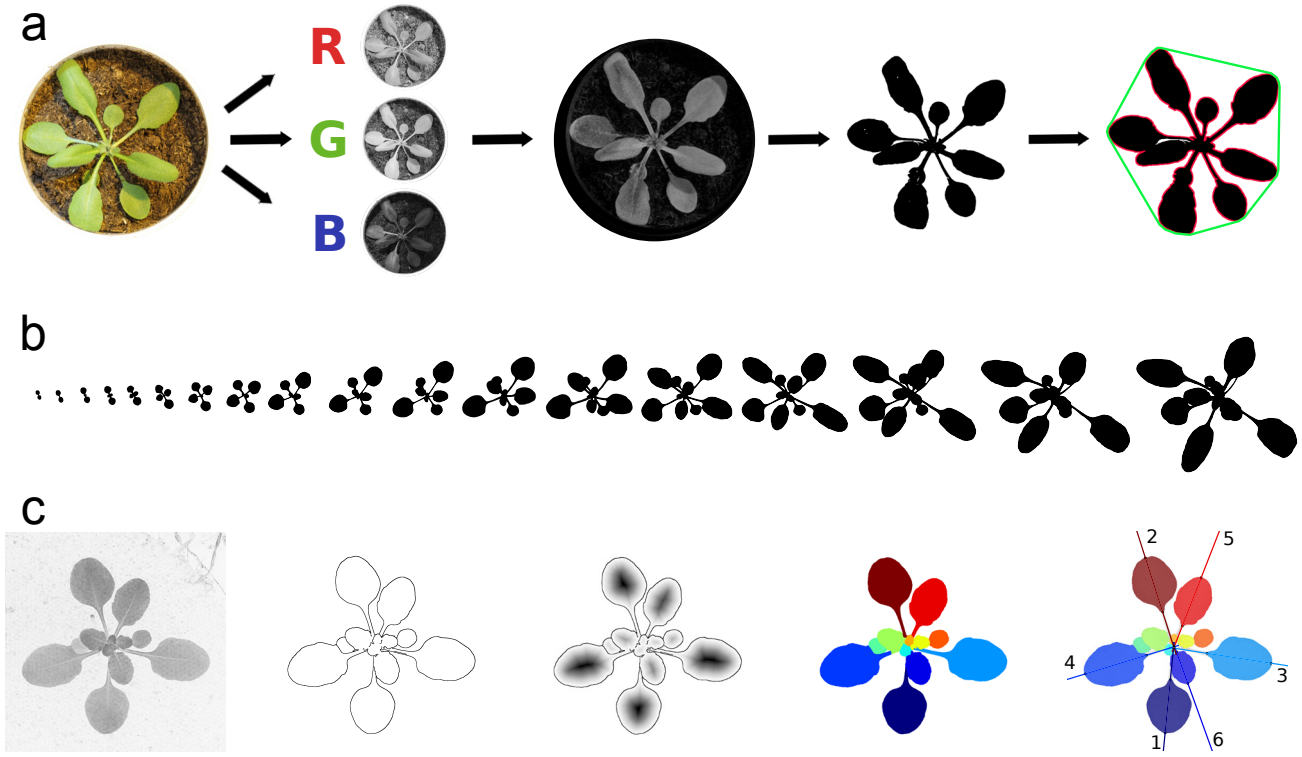

Figure 2. Non-destructive rosette imaging.

(a) Rosettes need to be isolated from the background using image segmentation, in this example, based on splitting the images in their red, blue and green (RGB) channels. The extracted binary representation of the rosette allows measuring different parameters, such as the projected rosette area (black), the convex hull (green) and the rosette perimeter (red). **(b)** Imaged over time, the rosette can be followed from the emergence of the cotyledons until bolting of the plants. Intrinsic to the spirally arrangement of leaves, only few overlap occurs. **(c)** From left to right: 2D focus image of an Arabidopsis rosette taken with the setup Phytotyping^{4D}, Sobel edge filtered image, Euclidian distance transform of the edge-filtered image, segmented rosette leaves of the distance transformed edge image, automatic assignment of leaves assuming leaves follow the golden angle (1-6: first 6 leaves) (Apelt et al., 2015).

Imaging beyond the visible spectrum

Both the temporal resolution and the dimensionality/data richness can be increased by imaging plants beyond the visible spectrum. Over the last years, several setups have been developed that take advantage of these spectra.

By combining near-infrared (IR) lighting, which is outside of the visible spectrum of plants, and a camera equipped with a daylight filter (and without the IR filter), plants can also be imaged during the night (De Vylder et al., 2012; Dhondt et al., 2014; Apelt et al., 2015), enabling the detection of differences in growth rate during the day and the night with an equivalent image exposure (Apelt et al., 2015).

Chlorophyll fluorescence imaging is widely applied in plant research to measure photosynthetic performance, also in high-throughput phenotyping systems (Jansen et al., 2009; De Vylder et al., 2012), and can be used to detect responses to abiotic and early biotic stresses (Chaerle and Van Der Straeten, 2000). For example, cold stress has been shown to negatively influence the photosynthetic efficiency in Arabidopsis, whereas plants exposed to drought stress do not show this photoinhibition (Jansen et al., 2009). Additionally, biotic stresses result in the downregulation of photosynthesis-related genes (Bilgin et al., 2010), leading to a reduction of photosynthetic efficiency. Therefore, early and late stages of pathogen infections can be visualized and quantified directly using fluorescence imaging by measuring the effect on the photosynthetic apparatus (Chou et al., 2000; Matouš et al., 2006; Berger et al., 2007).

Infrared thermal imaging provides information about the temperature emitted from leaf surfaces, which is influenced by evaporation and transpiration of leaves. The temperature of the leaf surface can therefore serve as a proxy for transpiration and stomatal conductance. The use of IR thermal imaging has led to the identification of Arabidopsis mutants that are defective in stomatal closure regulation (Merlot et al., 2002). Combining chlorophyll fluorescence and thermal imaging can provide insights in the water use efficiency of plants (McAusland et al., 2013).

Hyperspectral imaging collects information across the electromagnetic spectrum, beyond the limits of the human eye and standard cameras. According to their composition, different ma-

Box 1 - Rosette parameters and calculations

Projected rosette area: The projected rosette area represents the area that is occupied by the rosette in a top-view image (Figure 2a). The rosette area is extracted from images after picture segmentation and removal of the background. Due to overlap of the rosette leaves and leaf curvature, the projected rosette area will differ from the summation of the areas of its dissected leaves.

The convex hull of the rosette: The convex hull is the area defined by the smallest convex set containing the rosette. Easily stated, the convex hull can be considered as the area within a virtual rope wrapped around the rosette (Figure 2a). The size of the convex hull thus depends on the length of the leaf and petioles.

Rosette perimeter: The rosette perimeter is the length of the outline of the rosette (Figure 2a).

Stockiness: Stockiness is a mathematical measure of the roundness of the rosette and is calculated as followed:

$$Stockiness = 4\frac{\pi \times area}{perimeter^2}$$

A perfect round object will have a stockiness of 1, whereas more irregular objects will have lower values.

Surface coverage: Surface coverage, also referred to as compactness of a rosette, describes the ratio between the projected rosette and the convex hull. This value indicates how much of the surface of the convex hull is occupied by the rosette. Plants carrying a lot of leaves with short petioles will have a high surface coverage.

terials leave a unique spectral signature at different wavelengths, enabling their identification. Hyperspectral imaging has already been proven to be successful as a non-invasive technique in plant research for various purposes, such as mapping of leaf water content, analysis of the distribution of nitrogen and detection of peroxidase activity (Higa et al., 2013; Kong et al., 2014; Yu et al., 2014). Hyperspectral imaging only recently became available for indoor measurements and such systems are finding their way in laboratory research. In Arabidopsis, this technology has been applied to identify mutants with a different pigment content, which could not be identified by analysis of visible color or morphological changes (Matsuda et al., 2012). This technology is therefore very promising and its full potential has not yet been reached, because the interpretation of the different spectral bands is not straightforward. To analyze the combinations of different spectra and give a biological meaning to observed differences, substantial calibrations and optimizations of the used wavebands are required (Matsuda et al., 2012).

Some plant genotypes exhibit an extensive leaf curvature/waving (Palatnik et al., 2003; White, 2006) or affect only a subset of the rosette leaves at a certain timepoint (Gonzalez et al., 2010), which can lead to biased conclusions when only phenotyping the rosette. To gain further insights into leaf growth characteristics, more detailed analyses at the leaf organ level are required.

IMAGING AND MEASURING INDIVIDUAL ROSETTE LEAVES

From the rosette to the leaf: individual leaf segmentation

High-throughput and non-destructive imaging makes phenotyping the complete Arabidopsis rosette a widely used screening method to detect and quantify plant growth characteristics, but the spatial resolution remains limited. Overlap of growing leaves, although limited in Arabidopsis, can result in underestimations of the actual rosette size by only measuring the projected rosette area. To increase the resolution from the entire plant to the leaf level, leaves need to be isolated from the rosette. Classically, this is achieved by physically dissecting the rosette leaves, but it is also possible to estimate the leaf area or to segment the leaves from rosette images. The leaf area can be estimated based on the leaf radius, defined as the length from the leaf tip to the center of the rosette, and the curvature on the leaf tip (Tessmer et al., 2013). However, this method may fall short for plants with an altered petiole length or extensive leaf curvature.

The segmentation of individual leaves from rosette images and leaf number attribution is a challenging task (Janssens et al., 2013; Pape and Klukas, 2014), especially for small and overlapping leaves. However, Apelt et al. (2015) have achieved marking individual leaves by applying Euclidian distance transformations on the outline of leaf edges extracted from rosette pictures, followed by a smoothing of these distance-transformed images restricted to the segmented plant area (Figure 2c). In addition, individual leaf positions could be determined with the assumption that a phyllotactic pattern between subsequent leaves follows the “golden angle” (~137.5°). In addition to leaf overlap, hyponasty needs to be taken into consideration when measuring rosette size from images at a sub-daily resolution, because this can affect the projected rosette area. By combining focused and depth rosette images, a 3D rosette surface can be reconstructed, which enables measuring the plant area with a negligible effect of leaf angles (Apelt et al., 2015)

Physical or virtual dissections of leaves enable measuring total leaf number of the rosette and extracting individual leaf parameters, such as symmetry (Janssens et al., 2013), area, length, width (Gonzalez et al., 2010) and the ratio between the latter two: the leaf index (Tsukaya, 2002). Arabidopsis rosette leaves differ in size and morphology between different accessions (Pérez-Pérez et al., 2002), but also within the same plant of a given accession, a phenomenon referred to as heteroblasty (Tsukaya, 2002; Poethig, 2013; Tsukaya, 2013a) (Figure 3a). The first, juvenile Arabidopsis leaves are small, round-shaped and bear trichomes only at the adaxial side. The larger, narrower adult leaves bear trichomes at both adaxial and abaxial sides and have more serrations (Kerstetter and Poethig, 1998; Tsukaya, 2013a). In-depth studies of leaf growth dynamics mostly focus on one particular rosette leaf. The selection of this leaf depends on the observed phenotype (Gonzalez et al., 2010) and on the experimental setups. To study the earliest stages of leaf development, the first appearing leaves are more accessible to dissect and measure or examine *in vivo* with confocal microscopy (Kuchen et al., 2012) than the older leaves. In contrast, older leaves are sometimes chosen to avoid potential seed effects on leaf growth. Therefore, different research groups often focus and specialize on a particular rosette leaf (Donnelly et al., 1999; Granier et al., 2006; Andriankaja et al., 2012; Kalve et al., 2014b).

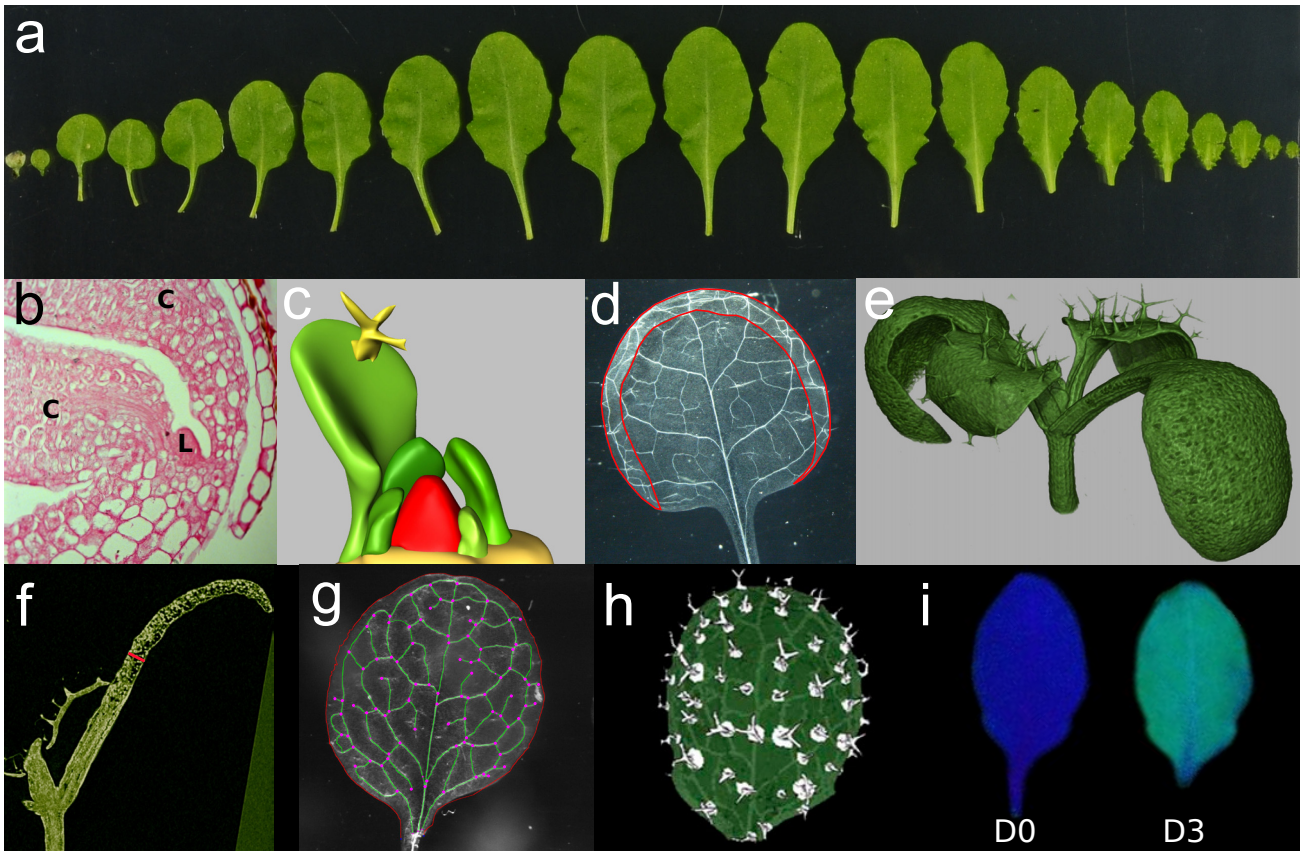

Figure 3. Quantitative phenotyping of the rosette leaf.

(a) Heteroblasty within an Arabidopsis rosette (accession C24). At the left, two embryonic cotyledons precede the true leaves; leaves are arranged from left to right in order of emergence from the SAM. **(b)** The first leaves (L) appear between the two cotyledons (C) at 3 DAS. **(c)** Using 3D reconstructions of leaf primordia, volumes of primordia that are otherwise difficult to access can be measured. **(d)** Transparent ethanol-cleared leaves allow visualization of the vasculature and more accurate measurements of leaves with a strong blade curvature (red). **(e)** Using HRXCT scanning, 3D representations of seedlings and leaves can be reconstructed from optical sections **(f)** in which leaf thickness (red) can be measured. **(g)** Total vascular system (green), branching points (purple dots) and the leaf perimeter (red) can be extracted semi-automatically from cleared leaves. **(h)** Trichome extraction and patterning in a developing leaf using optical projection tomography (OPT) (Lee et al., 2006). **(i)** The photochemical efficiency of PSII of leaves is high before a dark treatment (D0), represented by the dark-blue color. After 3 days of dark induced senescence (D3) treatment, this photochemical efficiency is lower, visualized by the light-blue color and yellow patches.

Quantifying leaf size in three dimensions

Leaf primordia initiate at regular positions from the peripheral zone of the SAM. These initiation patterns, resulting in the spiral phyllotaxis, are determined by local auxin maxima (Bayer et al., 2009). At 3 days after stratification (DAS), the primordia of the first leaf pair can be discriminated from the SAM (Figure 3b). After 5 DAS, the third leaf emerges and is quickly followed by the fourth. Due to this rapid succession, developing leaves are extensively covering the vegetative SAM and the younger leaf primordia, making imaging and quantifying the size of these small leaves challenging. Both optical and histological sectioning methods combined with 3D reconstruction of the images exist to visualize (Lee et al., 2006; Wuyts et al., 2010; Vlad et al., 2014) and measure the volume of leaf primordia (Vanhaeren et al., 2010) during their earliest stages of development (Figure 3c). Later during development, starting from 3-4 days after initiation (DAI) petioles start differentiating (Kalve et al., 2014b), and leaves can be micro-dissected from the apex with micro-scissors or hypodermic needles. After clearing, these dissected leaves are mounted on slides and imaged using a camera mounted on a binocular microscope, allowing accurate measurements of the leaf blade area regardless of leaf curvature and folding (Figure 3d).

In addition to leaf length and width, leaf thickness increases during the course of leaf development, albeit at a slower rate than the planar dimensions, explaining the flattened leaf morphology (Kalve et al., 2014b). Leaf thickness is determined by dorso-ventral leaf expansion, which is influenced by both genotype and environment (González-Bayón et al., 2006; Wuyts et al., 2012; Kalve et al., 2014b). To assess overall leaf thickness, histological (Beeckman and Viane, 2000; Kalve et al., 2014b)

and optical sectioning methods, such as multi-photon microscopy (Wuyts et al., 2010) and high-resolution X-ray computed tomography (HRXCT) (Figure 3e,f) (Dhondt et al., 2010) can be used.

Leaf growth parameters

Although single timepoint measurements can give indications of plant or leaf size, it does not allow calculating growth-related parameters (Box 2), which require measurements at multiple timepoints. Such measurements are mostly performed with a fixed time interval. Leaf area from early timepoints until maturity typically displays a sigmoidal curve. Since the area of mature leaves is several orders of magnitude larger than that of leaf initials, these data are generally plotted on a logarithmic scale to allow a better discrimination between genotypes or treatments, especially at early timepoints. Intrinsic to the underlying cellular processes driving growth, Arabidopsis leaves increase in size at different rates until leaf maturity is reached. These growth patterns can be described using several parameters, such as relative and absolute growth rate (RGR and AGR) and growth acceleration (Box 2). The ratio of the area of a leaf to its size on a previous timepoint corresponds to the RGR, whereas AGR reflects the area that is formed during a certain unit of time. The leaf measurements at different timepoints can be fitted with a local quadratic function or a complete curve fitting, allowing smoothing of the growth curve. The first order derivative of this smoothed curve, the AGR, is a measure of growth speed on that timepoint, representing the change of growth over time. The second order derivative of this smoothed growth curve gives the growth acceleration, corresponding to the change of this growth rate (Tessmer et al., 2013).

The biological meaning of these mentioned parameters can be illustrated as follows. During normal leaf development, the area of an initiating leaf primordium almost doubles in a single day; this is hence reflected in a high RGR. Later during development, these fold changes decline and the RGR will hence decrease over time. The absolute size of a leaf increases the most in the middle of its active growth period. Therefore, the AGR of leaves will reach a peak at this timepoint and typically displays a bell-shaped curve. Positive and negative values of growth acceleration indicate that the AGR is enhanced or decreased, respectively. For example, upon transfer of plants grown on control medium to medium containing osmotic compounds (Skirycz et al., 2011a), a negative growth acceleration reflects a reduction in growth rate compared to control conditions. These different growth-related parameters provide complementary views of the leaf growth dynamics in variable genetic backgrounds and environmental conditions.

Quantifying carbon assimilation and distribution in leaves

In leaves, carbon is fixed via the Calvin cycle, supplying the energy and building blocks for plant growth (Streb and Zeeman, 2012). Young leaves are unable to assimilate carbon and are not self-sustainable until chloroplasts start differentiating and the photosynthetic activity is switched on. These young leaves therefore depend on the import of carbon in the form of sugars from older leaves, creating a source-sink relation. In leaves, assimilated carbon is distributed to structural components, such as proteins and cell wall material, and to energy storage such as starch. Several methods exist to visualize and measure starch content and the carbon distribution between and within leaves. Starch content can be visualized using iodine staining and quantified by the enzymatic hydrolysis of starch to glucose. By $^{14}CO_2$ labeling, starch biosynthesis rates and turnover (Hostettler et al., 2011) and the allocation and partitioning of carbon in leaves (Kölling et al., 2013) can be measured. Using this method, older leaves that act as a carbon source have been shown to invest more in starch than in proteins and cell wall, whereas younger sink leaves partition assimilated carbon equally (Kölling et al., 2015). In addition, at the beginning of the day, more carbon is transferred from source leaves to the sink tissues than at the end of the day. Similar to the assimilated carbon, the imported carbon is equally distributed between starch, proteins and cell wall components in these young leaves (Kölling et al., 2015).

Box 2 – Rosette/leaf growth measurements

Leaf area over time: Measurements of the rosette/leaf blade area over different timepoints, mostly with a fixed interval, can be used to calculate various growth parameters. Since the area of mature leaves is several orders of magnitude larger than those of leaf initials, these data are generally plotted on a logarithmic scale.

Absolute growth rate (AGR): The absolute growth rate, sometimes referred to as growth velocity, corresponds to the plant area that is formed during a certain unit of time. From the growth curve, the measured timepoints are fitted with a local quadratic function, allowing smoothing of the curve. The first order derivative of this smoothed curve is the growth velocity on that timepoint. In leaves, the absolute growth rate increases and reaches a peak in leaves that are in the expansion phase.

$$AGR = \frac{A_t - A_{t-\Delta t}}{\Delta t} = \frac{dA(t)}{dt}$$

Relative growth rate (RGR): The ratio of a rosette or leaf to its size on a previous timepoint produces the relative growth rate. In non-destructive rosette imaging, this can be calculated for individual plants using the following formula:

$$RGR = \frac{ln(A_t) - ln(A_{t-\Delta t})}{\Delta t}$$

When using destructive measuring methods, this value can be calculated with the mean logarithmic transformed values of pooled samples for each timepoint (Hoffmann and Poorter, 2002):

$$RGR = \frac{\overline{ln(A_t)} - \overline{ln(A_{t-\Delta t})}}{\Delta t}$$

Growth acceleration: Growth acceleration is defined as the rate of change in absolute growth rate and is hence calculated as the second order derivative of the smoothed growth curve.

$$Acceleration = \frac{dA^2(t)}{dt^2}$$

Extracting leaf vasculature and trichome patterns

Procambial cells, the progenitors of vascular tissue, can already be detected during early leaf development (Mattsson et al., 1999; Turner and Sieburth, 2003). Analogous to heteroblasty, different rosette leaves within an accession (González-Bayón et al., 2006) and equivalent leaves from various accessions display different venation patterns (Candela et al., 1999). Quantification of leaf venation parameters are facilitated by dark-field images of cleared leaves, in which lignified mature xylem vessels stand out due to their light-scattering properties. These high-contrast pictures can be analyzed manually (Candela et al., 1999; González-Bayón et al., 2006; Rolland-Lagan et al., 2009) or with semi-automated analysis methods, such as LEAF GUI and LIMANI (Price et al., 2011; Dhondt et al., 2012). Different parameters can be extracted from these images, such as the total vascular length, vascular complexity (sum of the number of endpoints, branching points and vascular elements) and vascular density (vein length per unit leaf area) (Figure 3g). Throughout leaf development, the length and complexity of the total vascular system increase, whereas vascular density reaches a peak around 14 DAS. Afterward, vascular density declines during further development, because the leaf blade continues to expand and the vascular system grows at a slower rate (Dhondt et al., 2012). Using vascular tissue-specific reporter lines, time-lapse imaging of vascular development can be performed by confocal laser scanning microscopy (CLSM) (Sawchuk et al., 2007). With optical projection tomography (OPT), venation patterns can be extracted using region-growing algorithms, resulting in 3D representations of the vasculature, from which vein volumes can be quantified (Lee et al., 2006). With the latter technique, it is possible to identify trichomes, which are specialized epidermal cells, to generate trichome distribution maps (Figure 3h). Similarly, trichome distribution can be measured using confocal imaging (Bensch et al., 2009) and HRXCT (Kaminuma et al., 2008).

The end of the line: leaf senescence

At the end of the Arabidopsis life cycle, mature leaves start senescing, enabling nutrient recycling and reallocation (Guiboileau et al., 2010). This process is governed by developmental, environmental and hormonal signals (Khan et al., 2014). Senescence is characterized by yellowing of the leaf and a reduction of the photosynthetic apparatus, phenomena that can be mimicked by a dark treatment of leaves, called dark-induced senescence (DIS) (Weaver and Amasino, 2001). DIS is a widely used phenotyping method to accelerate leaf senescence in a consistent manner (Oh et al., 1997). This process is commonly quantified by measuring the photochemical efficiency of photosystem II (PSII) using fluorescence imaging (Figure 3i). This phenotyping technique enabled for example the detection of genes playing a role in leaf senescence (Oh et al., 1997) and longevity (Debernardi et al., 2014).

Measuring different aspects of leaf growth and quantifying growth dynamics over time yield numerous insights into leaf development. Since a strict coordination of cell proliferation and expansion during leaf growth determines its final size, phenotyping leaves at the cellular level is required to further understand leaf growth in control conditions and upon genetic and environmental perturbations.

PHENOTYPING LEAF DEVELOPMENT AT A CELLULAR LEVEL

During leaf development, several interconnected processes controlling leaf size occur: i) cell proliferation, ii) meristemoid division and iii) cell expansion (Gonzalez et al., 2012) that can have different rates and durations.

From the SAM, leaf initials emerge, in which cells grow through cytoplasmic enlargement before mitotic division. Whereas in ferns, leaf blade development depends on a marginal meristem (Boyce, 2007), its contribution in Arabidopsis is still under discussion (Donnelly et al., 1999; Tsukaya, 2013a). The different axes that determine the flat morphology of Arabidopsis leaves are formed early on (for a review: Tsukaya, 2013a). Along the dorsoventral axis, specialized cell types are formed (Figure 4). The narrow adaxial and abaxial epidermal layers isolate the inner leaf tissues from the environment, allowing tightly controlled gas and water exchange through the stomata (Pillitteri and Dong, 2013), the pores in the epidermis, of which the opening is controlled by specialized guard cells. The majority of photosynthesis occurs at the adaxial side of the leaf, in the pallisade parenchyma. Gas exchange primarily happens at the abaxial orientated spongy mesophyll, explaining the larger intracellular spaces between spongy parenchyma cells and the higher stomatal density of the abaxial epidermis (Figure 4). This specialized cellular arrangement allows a maximal photosynthetic efficiency, while water losses are reduced to a minimum. Facilitated by this planar morphology of growing leaves, numerous techniques exist to visualize and quantify cellular characteristics.

Reporter lines to study growth

Fusing reporter genes, such as β-glucuronidase (GUS) and the green fluorescent protein (GFP), to specific promoters has considerably advanced our knowledge of the localization, dynamics and timing of the cellular processes driving leaf growth. The GUS reporter system is a destructive method based on the enzymatic conversion of glucuronide substrates, from which 5-bromo-4-chloro-3-indolyl glucuronide (X-Gluc) is most frequently used, into a colored precipitate (Janssen and Gardner, 1989). The strength of the colored signal is influenced by the incubation period, but also by the used promoter-GUS construct depending on the strength of the promoter, and by the penetration efficiency of the substrate in the plant tissue. For example, one promoter-GUS construct can lead to overstaining after six hours of incubation, whereas another could show no signal at all. GUS staining is usually visualized with dark-field or light microscopy on entire leaves or on histological sections (Donnelly et al., 1999). Three dimensional visualization of gene expression patterns using OPT can also be obtained by combining fluorescence OPT to detect the tissue of a specimen and transmission OPT using visible light to determine *GUS*-expressing regions (Lee et al., 2006). Reporter

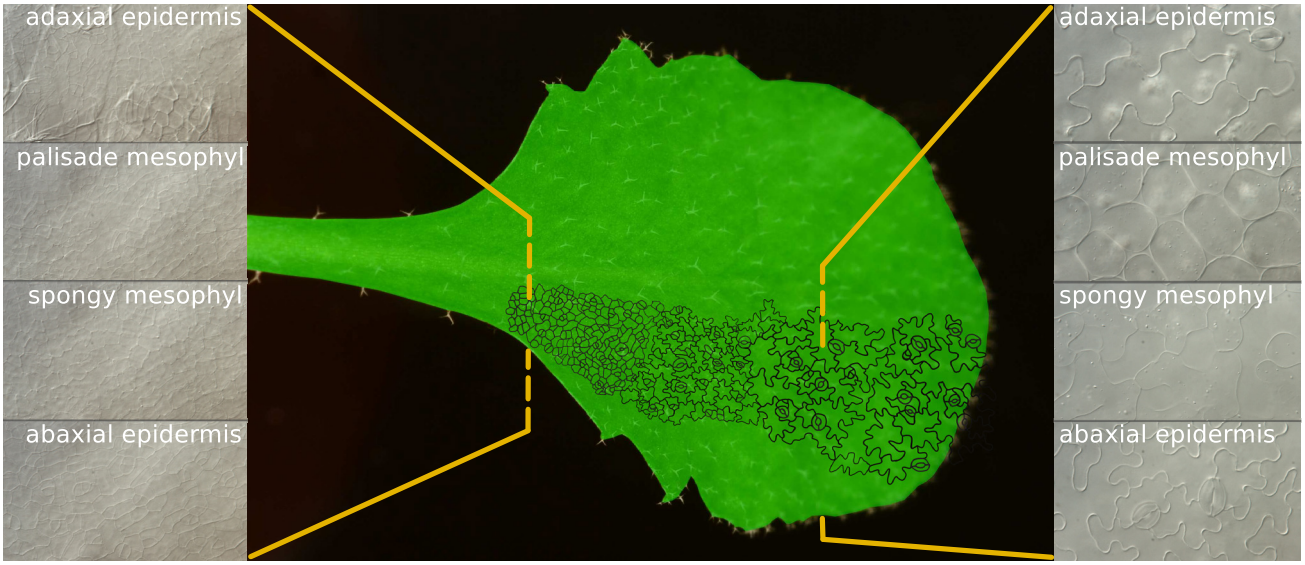

Figure 4. Cell differentiation during leaf development.

Along the proximal-distal axis of the leaf, a cell cycle arrest front proceeds in a basipetal direction, coinciding with cell differentiation. Along the dorso-ventral axis (insets at the left and right), specialized cell layers fulfill distinct functions and display different morphological traits, which are the clearest in differentiating parts of the leaf.

lines enable detection of tissue-specific gene expression in the leaf, but also the analysis of the timing of cellular processes. By studying plants that carry the *pCYCB1;1::GUS* reporter construct with a cyclin destruction box, ensuring degradation of the GUS protein at the end of each mitosis, the transition from cell proliferation to cell expansion could be quantified (Donnelly et al., 1999). This transition starts at the tip of the leaf, where cells stop dividing and start differentiating and expanding. This cell cycle arrest front proceeds along a proximal-distal axis (Figure 4), but the exact timing of the cell cycle arrest differs between the epidermal and mesophyll layers (Donnelly et al., 1999). Additional research studies on this transition event using *pCYCB1;1::CYCB1;1::GUS* and *pKLU::GUS* reporter lines have shown that the cell cycle arrest front does not proceed gradually, but is rather held at a same position after initiation until it rapidly moves toward the base of the leaf (Kazama et al., 2010). In addition, the use of *pCYCB1,1::GUS* has led to the proposition of a second arrest front that regulates the activity of dispersed meristemoid cells (White, 2006). These small cells continue to divide asymmetrically and give rise to additional pavement cells and stomata.

In addition to the *pCYCB1;1* mitosis-specific marker, other marker lines specific for hormones, such as *pDR5::GUS* (Ulmasov et al., 1997) and reporter lines specific for trichomes, stomata, vasculature, leaf mesophyll and epidermal layers, can be used to visualize and quantify leaf growth characteristics (Lee et al., 2006; Sawchuk et al., 2007; Mustroph et al., 2009).

In vivo confocal microscopy can give more insights into the subcellular protein localization using translational GFP fusions. In contrast to roots which lack chloroplasts, confocal and multi-photon imaging of leaves can be complicated by the presence of chlorophyll that interferes with the fluorescence signals (Cheng et al., 2001). Reporter lines with a strong GFP signal that can be distinguished from background auto-fluorescence are powerful tools to study leaf growth (Sawchuk et al., 2007; Kuchen et al., 2012). For example, by using plasma membrane-targeted GFP markers, cell division in the first leaf pair was followed *in vivo* with a confocal microscope and enabled computational modeling of early leaf growth (Kuchen et al., 2012). *In vivo* imaging of cells is however limited, since the illumination of the sample eventually causes cell damage (Cheng et al., 2001).

Quantifying cellular processes that underlie leaf growth

The movement of the cell division arrest front during leaf development was confirmed by an extended phenotypical study of the transition from cell division to cell expansion (Andriankaja et al., 2012). In this study, microscopic drawings along the entire abaxial epidermis of cleared leaves were produced using a differential interference contrast (DIC) microscope (also known as Nomarski microscopy) equipped with a drawing tube (Nelissen et al., 2013). Such cell drawings can be digitalized and processed using automated image analysis scripts (Andriankaja et al., 2012) (Figure 5a), but they can also be analyzed manually using ImageJ (Nelissen et al., 2013). The major advantages of using cleared leaves for cellular profiling are that underlying mesophyll cell layers can also be measured (Ferjani et al., 2007) and that the same leaf material can be used to measure leaf area and vasculature (see 'Imaging and measuring rosette leaves'). Another approach to visualize and quantify cell divisions uses aniline blue staining

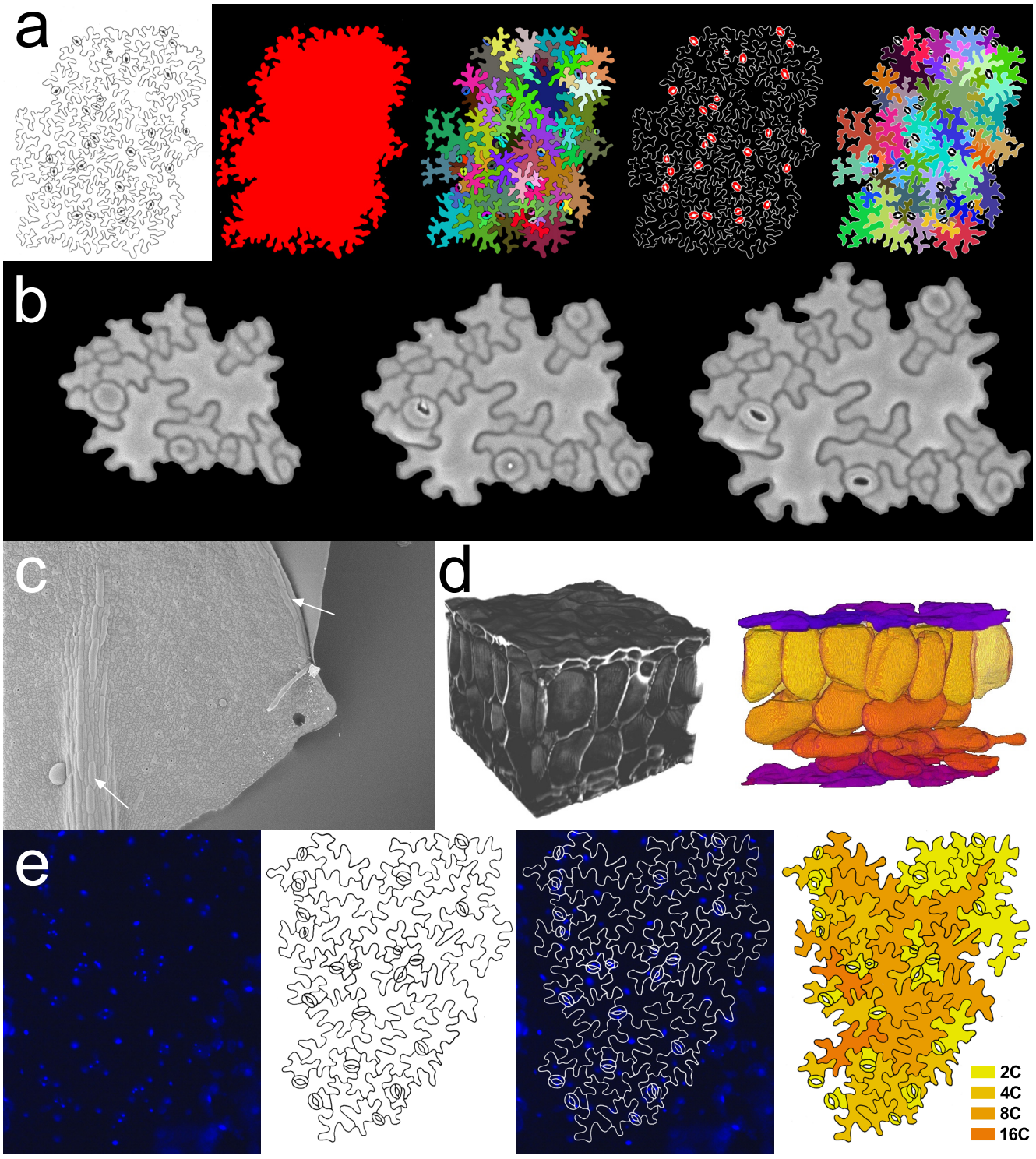

Figure 5. Cellular phenomics of leaf growth.

(a) Analysis of digitalized epidermal cell drawings using automated image analysis scripts that extract the surface of the drawn area, cell area, stomatal count and pavement cell area (Andriankaja et al., 2012). (b) Non-destructive imaging of dividing and expanding cells over different timepoints using dental resin imprints. (c) Enlarged and elongated cells above the midvein cells and in close proximity to the leaf border. (d) Multi-photon image stacks and 3D reconstructed cell volumes across the different cell layers. The adaxial (upper) and abaxial (lower) epidermal layers are displayed in purple, the cylindrical palisade parenchyma cells are colored in yellow and the irregular shaped spongy parenchyma cells are colored in darker orange to red (Wuyts et al., 2010). (d) Nuclei of epidermal peels visualized with a fluorescence microscope after DAPI staining (blue). Combined with cellular representations of these peels, endoploidy maps can be made. Cells with 2C nuclei are marked in yellow, orange cells have nuclei with a higher ploidy level.

of callose in the newly formed cell walls. This staining can be visualized using a fluorescence microscope, but trichomes need to be removed to avoid interference with the fluorescence signal (Kuwabara et al., 2011).

With imprinting techniques, the leaf epidermis can be visualized and cell size-related parameters can be quantified non-destructively. Agarose-mediated imprints can be analyzed directly using DIC microscopy (Mathur and Koncz, 1997; Christensen, 2010) and dental resin imprints or nail polish replicas generated from these molds can be imaged using a light and/or scanning electron microscope (SEM) (Figure 5b) (Geisler et al., 2000). Using the latter method, cellular dynamics of a single leaf have been followed for up to 12 successive timepoints to track asymmetric divisions of meristemoid cells (Geisler et al., 2000). Such successive imprints can provide detailed insights into the duration, extent and patterning of cell division and expansion (Figure 5b) (Elsner et al., 2012). Using epidermal imprints, the differentiating puzzle-shaped pavement cells have been shown to occasionally divide, even after differentiation was initiated (Elsner et al., 2012).

Various cellular parameters, such as average cell area, cell number, cell circularity, number of stomata, stomatal index and stomatal density, and the cell area distribution (Box 3) can be extracted from these images. From cellular data obtained at different timepoints, cell division and expansion rates can be derived (Box 3). For all cellular analyses, care needs to be taken that regions above the midvein and the border of leaves are avoided, because in these regions, cells are much larger and display different characteristics than other cells of the leaf blade (Kawamura et al., 2010) (Figure 5c). These cells appear already early during development and cover a relatively large proportion of the total leaf area. Later during development, this proportion is reduced, because the leaf blade continues to expand. Their exact function apart from providing ruggedness to the leaf remains unclear. Since cell division is arrested in a tip-to-base gradient, it is also necessary to do two measurements at specific positions in the immature leaf: one at a quarter from both the base and tip of the leaf and another halfway between the leaf margin and the midvein of growing leaves (Nelissen et al., 2013).

Next to the epidermal cell layers, the palisade parenchyma is often used to quantify cellular parameters (Horiguchi et al., 2006). The major advantage of this tissue is that its cells are very uniform in shape and size compared to those of the epidermal layers (Figure 4), because they lack cells of the stomatal cell lineage. However, they are more challenging to access and intercellular spaces are found between the cells (Figure 4). DIC microscopy on cleared leaves, as described above, is a very straightforward method to measure the area the palisade parenchyma cells. Since palisade cells are cylindrically elongated, and spongy parenchyma cells can show irregular shapes, histological transverse sections through the leaf (Kalve et al., 2014b) and measurements of cell volumes using multi-photon microscopy (Figure 5d) (Wuyts et al., 2010; Wuyts et al., 2012) provide

Box 3 – Cellular measurements and calculations

Cellular measurements, calculations and statistics are commonly performed on a specific cell layer. The abaxial epidermis, since juvenile leaves lack hindering trichomes on this side, or the palisade mesophyll are mostly chosen for this. For the definitions below, we used the abaxial epidermis as an example.

Average cell area: The average cell area of a leaf comprises both pavement cells and stomatal guard cells. The small size of the latter will result in a skew distribution to the right in maturing leaves, since the size of the expanding pavement cells will be much larger than the mean (Figure 5a, picture 3). Within a defined area of the leaf, cell areas are measured, from which an average area is calculated. Alternatively, the area in which cells are counted (Figure 5a, picture 2) can be divided by the total number of cells in that area. This method produces however an estimate of the average cell size and does not yield the actual distribution of the cell sizes.

Average pavement cell area: The average pavement cell area can be calculated analogously to that of the average cell area with the exception that the area of guard cells is not taken into account (Figure 5a, picture 5).

Total cell number/pavement cell number: The total cell and pavement number per leaf can be calculated by extrapolating the total cell number or pavement cell number, respectively, per drawn area (Figure 5a, picture 2) to the total leaf area.

Stomatal density (SD): The SD is defined as the number of stomata per mm^2 of leaf area. This value is dependent on the total amount of stomata and the size of the epidermal cells.

Stomatal index (SI): The SI describes the number of stomata compared to the total number of cells, hereby normalizing for the size of the epidermal cells.

$$SI = \frac{Number\ of\ stomata}{Number\ of\ epidermal\ cells + Number\ of\ stomata} \times 100$$

Cell division and expansion rate: Rates of cell division ($\frac{\frac{cells}{cells}}{t}$) and cell expansion ($\frac{\frac{cellarea}{cellarea}}{t}$) are calculated as the relative rate of increase in cell number and cell size over time, respectively. For this, the logarithmic values of means of cell number or cell size of the measured timepoints are fitted with a local quadratic function, allowing smoothing of the curve. The first derivative of these smoothed curves can be used as the relative division and expansion rates.

Cell cycle duration: Cell cycle duration is calculated as the inverse of the cell division rate.

Cell size distribution: Cell size distributions can be represented in frequency tables, in which the count of cells within a defined size interval is displayed. This representation allows for a more detailed interpretation of the cellular data than a single value, such as the average cell area, and enables a straightforward detection of shifts in cell size.

additional information about the contribution of these cell layers to the leaf biomass.

Cell expansion and endoreduplication

The absolute growth of leaves is the highest when the majority of cells are maturing and expanding. Whereas in proliferating tissue, the expansion of cells is established by cytoplasmic growth and doubling of nuclear DNA, the increase in cell volume of differentiating cells is driven by turgor pressure. This cellular expansion is established by several processes. First, a controlled modification of the cell wall, resulting in cell wall relaxation, combined with an increase in the vacuole size, drives cell wall deformation. Then, the cell wall is stiffened by cross-linking and new cell wall material is secreted (Cosgrove, 2005). Turgor pressure, the main driving force of this cellular growth, can be monitored in single cells by puncturing the cell wall using pressure probes (Green and Stanton, 1967). This method is conventional, but is however destructive and does not allow measuring the pressure in small cells, because their volume is not sufficient to reach the required equilibrium between the sap entering the probe and the remaining volume in the punctured cell (Green and Stanton, 1967). The thickness of the Arabidopsis cell wall, the elastic modulus of the cells and the turgor pressure can be measured *in vivo* using nano-indentations (Forouzesh et al., 2013).

Leaf cell expansion and differentiation coincides with an increase in endoreduplication, also known as endoploidization, which is the doubling of chromosomal DNA in the absence of chromosome separation and cytokinesis (De Veylder et al., 2001). During early leaf development, the majority of cells is mitotically active; these leaves are therefore predominantly composed of 2C and 4C nuclei-containing cells. Later during development, ploidy levels can reach up to 32C through endoreduplication. Although endoreduplication levels are hence often used as developmental markers, a causal relation between endoreduplication levels and cell size is still unknown (Tsukaya, 2013b). Endoreduplication can be measured using flow cytometry, a method allowing the measurement of DNA content by quantifying the fluorescence of nuclei stained with the DNA-specific fluorochrome 4',6-diamidino-2-phenylindole (DAPI) (Nelissen et al., 2013). This approach pools all different cell layers of the entire leaf, giving general insights into endoploidy levels on the organ level at a certain timepoint or over time. To correlate individual cell size with its ploidy level, the area of epidermal cells and the relative fluorescence of their DAPI-stained nuclei can be measured by isolating this cell layer using epidermal peels (Melaragno et al., 1993) (Figure 5e).

Cell proliferation, cell expansion and the coordination between these two processes by complex networks of genes determine the final shape and size of a leaf. Therefore, links between the macro- and microscopic phenotype and the underlying genetics can be made by phenotyping leaf growth on the molecular level.

MOLECULAR PHENOTYPING OF LEAF DEVELOPMENT

From initiation to maturation, different cellular processes coordinate leaf growth. These cellular events are regulated by complex networks of genes (Gonzalez et al., 2012; Tsukaya, 2013a; Hepworth and Lenhard, 2014; Kalve et al., 2014a; Rodriguez et al., 2014). By molecularly phenotyping leaves during the different developmental stages, and studying mutants and transgenic lines that alter final leaf size, the molecular networks underlying leaf growth can be unraveled.

Profiling gene expression during leaf development

During primordium initiation and leaf axis formation, expression of different genes coordinates and determines tissue identity and leaf outgrowth (Tsukaya, 2013a). A combined cellular and molecular phenotyping study of developing leaves has shown that many genes display a gradual expression change during the transition from cell proliferation to expansion (Andriankaja et al., 2012). The expression of numerous genes which play a role in cell proliferation, such as *ANGUSTIFOLIA3 (AN3*; AT5G28640), *GROWTH-REGULATING FACTOR5* (*GRF5*; AT3G13960), *KLUH* (*KLU*: AT1G13710) and many cell cycle-regulating genes, is high in fully proliferating leaves, gradually decreases during the transition from proliferation to cell expansion and is found to be lower or even absent in leaves with predominantly expanding cells (Beemster et al., 2005; Andriankaja et al., 2012). Conversely, negative regulators of the mitotic cell cycle, such as *SIAMESE RELATED 1* (*SMR1*, AT3G10525), and genes encoding expansins are upregulated at the onset of differentiation compared to earlier stages of leaf development (Andriankaja et al., 2012). During the transition from cell proliferation to cell expansion, chloroplasts start differentiating and the photosynthetic machinery is switched on, coinciding with the greening of the tip of the leaves. When the differentiation of the photosynthetic apparatus is blocked, cell expansion is inhibited, suggesting a link between cell differentiation and photosynthesis (Andriankaja et al., 2012).

For molecular phenotyping, the choice of the sampled material largely influences the resolution. Obviously, by profiling the transcriptome of isolated leaves, more development-specific growth regulators can be identified than when total seedlings are used. For example, by comparing the effect of osmotic stress on proliferating, expanding and mature leaves to that of whole seedlings, it was shown that almost none of the transcriptional changes that occurred exclusively in proliferating and maturing leaves could be retrieved in whole seedling samples (Skirycz et al., 2010). Even when micro-dissected leaves are sampled, various tissues and different cellular stages are pooled. Isolation of specific developmental zones of the growing leaf by laser dissection prior to transcriptome analysis (Inada and Wildermuth, 2005) can enhance the profiling resolution even further and can provide a better view of the transcriptional landscape in the leaf. This technique has already been successfully applied in leaves to study the transcriptome of provascular cells (Gandotra et al., 2013).

Other tissue-specific approaches use fluorescence-activated cell sorting (FACS) combined with transcriptome analysis or

FLAG-epitope tagged ribosomal protein L18 under the control of different tissue-specific promoters for translatome profiling. With the first method, epidermal cells and cells from specific stomatal lineage stages are isolated and profiled transcriptionally, providing a detailed stomatal lineage expression map (Adrian et al., 2015). Using tagged ribosomal proteins, ribosome-associated mRNAs are immuno-purified from specific cell populations of seedlings and hybridized against the Arabidopsis ATH1 Genome Array (Mustroph et al., 2009). Expression patterns of genes in specific cellular zones can be viewed in the online cell type-specific Arabidopsis electronic fluorescent pictograph (eFP) browser (http://efp.ucr.edu/). This Arabidopsis eFP browser integrates multiple transcriptome data sets and allows visualization of gene expression levels over a range of different leaf developmental stages and other plant organs (Winter et al., 2007) (http://bar.utoronto.ca/). Over the last years, transcriptome analyses were commonly done by hybridizing RNA samples onto the Arabidopsis ATH1 Genome Array, representing approximately 22,800 genes (Redman et al., 2004). RNA-sequencing uses direct sequencing of transcripts by deep sequencing technologies and is becoming increasingly popular because of its numerous advantages over microarray technology (Mutz et al., 2013).

Forward and reverse genetic screens

Forward and reverse genetics are often used to identify genes regulating leaf growth. Detecting new leaf growth regulators using forward genetic screens is not straightforward, since quantitative traits such as leaf growth are subjected to variation induced by environmental conditions. In addition, changes in growth caused by an altered gene expression level can often be subtle. However, mutations resulting in dramatic increases in leaf size have been described using this approach. The semi-dominant *GRANDIFOLIA-D* (*gra-D*) mutant has been identified by a genetic screen from a population of mutants generated through the use of irradiation. Genetic analysis of *gra-D* plants that produce very large leaves showed a large segmental duplication of the lower part of chromosome 4 (Horiguchi et al., 2009). Similarly, *DA1* (AT1G19270) has been identified from an ethyl-methanesulphonate (EMS) screen as a novel regulator of leaf and seed size. An additional screen of *da1-1* mutants treated with EMS identified the *ENHANCER OF DA1* (*EOD1*) (Li et al., 2008), which was found to be allelic to the previously described growth regulator *BIG BROTHER* (*BB*; AT3G63530) (Disch et al., 2006).

Next to forward genetic screens, a large-scale reverse genetics study on a collection of gene-indexed insertional mutants of Arabidopsis has recently been performed to identify genes involved in leaf development (Wilson-Sánchez et al., 2014). This screen resulted in the identification of 706 mutants exhibiting a leaf phenotype, such as changes in rosette and/or leaf lamina size, leaf shape and color. A publicly available database of this study can be queried using the web application PhenoLeaf (http://genetics.umh.es/phenoleaf).

Gene centric approaches

Phenotypic analysis of various mutants and transgenic lines that show an enhanced leaf size has allowed the identification of different pathways and numerous genes involved in the regulation of leaf growth (Gonzalez et al., 2009; Hepworth and Lenhard, 2014) (Figure 6a). For example, downregulation of *SAMBA* (AT1G32310) enhances the volume of leaf primordia in early stages of development (Eloy et al., 2012) and overexpression of *AN3* enhances both the rate of cell division and the duration of the cell division phase (Horiguchi et al., 2005; Lee et al., 2009). Similarly, overexpression of the brassinosteroid receptor, *BRASSINOSTEROID INSENSITIVE 1* (*BRI1*; AT4G39400), the transcription factor *GRF5* or the mi-RNA, *JAGGED AND WAVY* (*JAW*; AT4G23713), (Wang et al., 2001; Palatnik et al., 2003; Horiguchi et al., 2005) increases leaf cell number by extending the duration of cell division, resulting in an increased leaf area. On the opposite, both *DA1* and *EOD1* negatively regulate leaf size by limiting the duration of cell proliferation (Dish et al., 2006; Li et al., 2008). Mutations in these genes lead to the formation of larger leaves. Downregulation of the *PEAPOD1/2* genes (*PPD1/PPD2*; AT4G14713, AT4G14720) results in larger, dome-shaped leaves containing more cells, resulting from a prolonged period of meristemoid division (White, 2006). In *GIBBERELLIN 20-OXIDASE 1* (*GA20OX1;* AT4G25420)-overexpressing plants, both cell number and size are increased (Huang et al., 1998; Gonzalez et al., 2010). Cell size is positively regulated by *EXPANSIN 10* (*EXP10*; AT1G26770) and *SMALL AUXIN UP-REGULATED RNA19* (*SAUR19;* AT5G18010), because overexpression of these genes enhances cell expansion (Cho and Cosgrove, 2000; Spartz et al., 2012). In contrast, *SMALL AUXIN UP-REGULATED RNA36* (*SAUR36*; AT2G45210) negatively regulates cell expansion, because *saur36* mutants produce bigger leaves containing larger cells (Hou et al., 2013).

In conclusion, macroscopic and microscopic phenotypic analyses of mutants and transgenic lines with an enhanced leaf size allow extending our knowledge of the processes driving leaf growth. By molecularly profiling these mutants and wild-type plants, new components of the leaf growth regulatory network can be discovered. As a next step to dissect the complex leaf growth regulation pathway, connections between the genes and mechanisms regulating organ size can be found using a combinatorial approach (Vanhaeren et al., 2014). This study showed that synergism in leaf growth could be achieved by combining mutants that control similar cellular processes, such as cell division, but also by combining genes that drive cell division with those promoting cell expansion (Figure 6b). In addition, some growth-regulatory genes, such as *BRI1*, *SAUR19* and *SAMBA*, have been found to lead to a synergistic effect in the majority of combinations they were part of, suggesting they play a central role in the leaf growth regulatory networks (Vanhaeren et al., 2014).

CONCLUSIONS AND PERSPECTIVES

Plant growth is a quantitative trait, which is regulated by complex interconnected genetic networks. To unravel these mechanisms that control leaf growth, many research groups are constantly

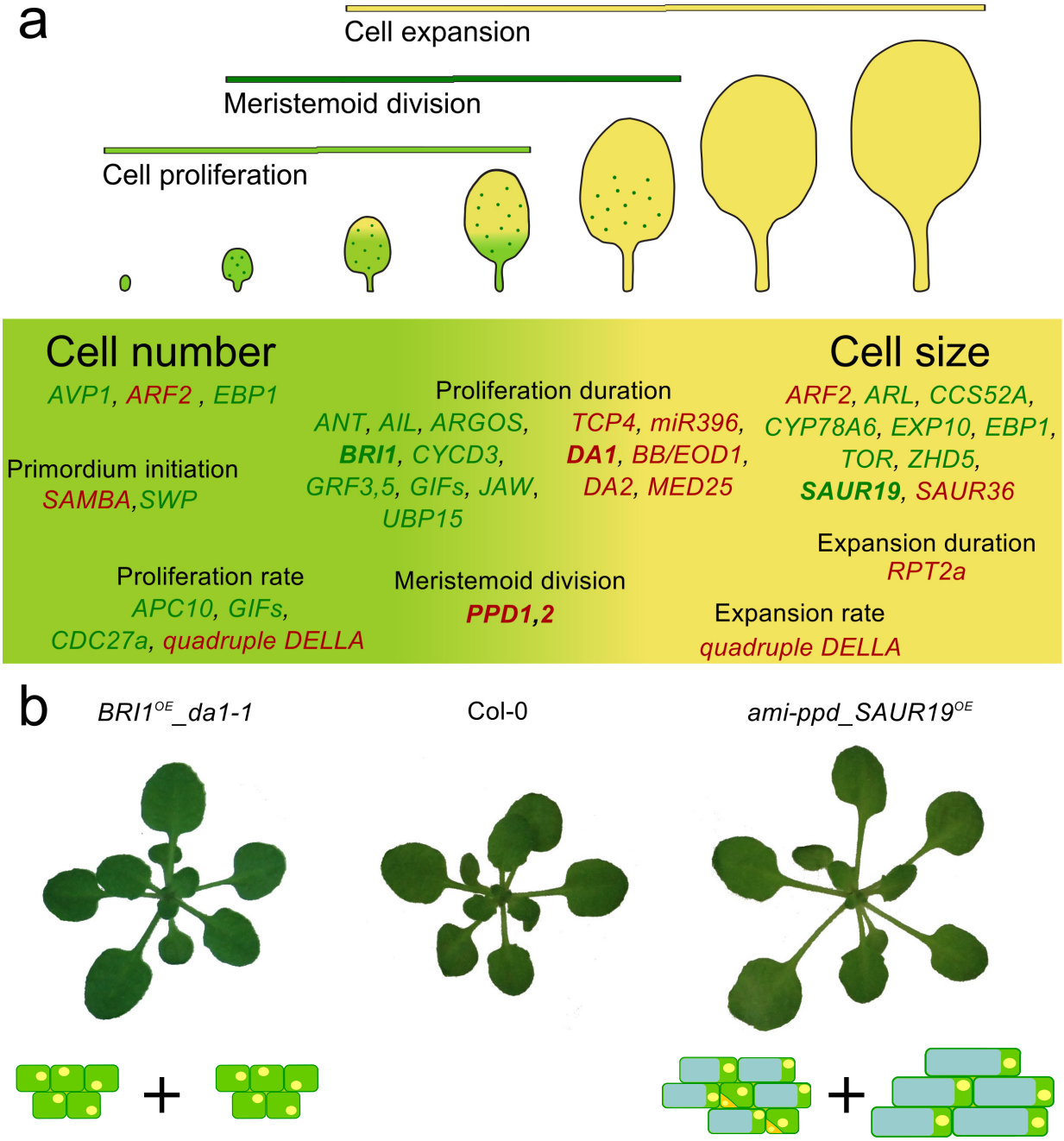

Figure 6. Molecular mechanisms regulating leaf size.

(a) The different processes that can influence cell number, cell size and hence final leaf size (i.e. primordium initiation, the duration of proliferation, the rate of proliferation, meristemoid division, cell expansion rate and cell expansion duration) are presented. These events are positively (green) and negatively (red) regulated by different genes. **(b)** Combinatorial approaches revealed that leaf size can be synergistically enhanced by combining genes controlling cell division (*BRI1^{OE}_da1-1*) and genes promoting cell (meristemoid) division and expansion (*ami-ppd_SAUR^{19}*). (Abbreviations: *ANT* (*AINTEGUMENTA*: AT4G37750), *APC10* (*ANAPHASE PROMOTING COMPLEX 10*: AT2G18290), *ARF2* (*AUXIN RESPONSE FACTOR 2*: AT5G62000), *ARGOS* (*AUXIN-REGULATED GENE INVOLVED IN ORGAN SIZE*: AT3G59900), *ARL* (*ARGOS-LIKE*: AT2G44080), *AVP1* (*ARABIDOPSIS THALIANA V-PPASE 3*: AT1G15690), CCS52A (AT4G11920) *CCS27A* (*CELL CYCLE SWITCH PROTEIN 52*, AT3G16320), *CYCD3* (*CYCLIN D3*), *DA2* (AT1G78420), *CYP78A6* (*CYTOCHROME P450, FAMILY 78, SUBFAMILY A*, AT2G46660) *EBP1* (*A. THALIANA ERBB-3 BINDING PROTEIN 1*: AT3G51800), *GIFs*: *GRF1-INTERACTING FACTOR 1,2,3*: AT5G28640, AT1G01160, AT4G00850), *GRF3* (*GROWTH-REGULATING FACTOR 3*: AT2G36400), *MED25* (*MEDIATOR 25*: AT1G25540), *miR396a* (*MICRORNA396A*: AT2G10606), *miR396b* (*MICRORNA396B*: AT5G35407), quadruple *DELLA* (*GAI* (*GIBBERELLIC ACID INSENSITIVE*: AT1G14920) *RGA* (*REPRESSOR OF GA*: AT2G01570) *RGL1* (*RGA-LIKE 1*: AT1G66350), *RGL2* (*RGA-LIKE 2*: AT3G03450)), *RPT2a* (*REGULATORY PARTICLE AAA-ATPASE 2A*: AT4G29040), *SWP* (*STRUWWELPETER*: AT3G04740), *TCP4* (*TCP FAMILY TRANSCRIPTION FACTOR 4*: AT3G15030), *TOR* (*TARGET OF RAPAMYCIN*: AT1G50030), *ZHD5* (*ZINC-FINGER HOMEODOMAIN 5*: AT1G75240), *UBP15* (*UBIQUITIN-SPECIFIC PROTEASE 15*, AT1G17110).

investing in the development of new phenotyping approaches and analysis tools (www.plant-image-analysis.org) to increase the spatial or temporal resolution and enhance the throughput by which plants can be analyzed. The use of robotics allows the automation of large-scale live imaging that would be very challenging to carry out manually. For example, automated growth platforms have enabled large screens of natural variants (Granier et al., 2006) and transgenic lines (Skirycz et al., 2011b) to study their growth response under water-limiting conditions.

Phenotypes can be used as readout for a plethora of traits, such as photosynthesis efficiency, nutrient deprivation and various biotic and abiotic stress responses. Increasing the resolution and dimensionality of automated high-throughput systems by, for example, realizing the segmentation of individual leaves from a rosette image (Apelt et al., 2015), combining measurements in different spectra (De Vylder et al., 2012) and enabling different irrigation regimes (Granier et al., 2006; Skirycz et al., 2011b; Tisné et al., 2013), can result in very rich data sets. Together with recent developments in large-scale sequencing, resulting in detailed genotyping information about different Arabidopsis accessions (Ossowski et al., 2008; Weigel and Mott, 2009; Cao et al., 2011; Gan et al., 2011; Schneeberger et al., 2011; Long et al., 2013; Schmitz et al., 2013), large-scale rosette growth, thermal and fluorescence phenotyping can now be used to assess the relation between the genotype and phenotype in these accessions and therefore allow the identification of novel genes regulating growth, resistance to pathogen infections and water use efficiency. Subsequently, detailed phenotyping of interesting candidates can further narrow down the time frame for molecular profiling to unravel the molecular basis of the initially observed traits. Various genome wide association (GWA) experiments have already been performed to study the natural variation explaining various sets of quantitative root growth traits using high-throughput imaging systems in Arabidopsis (Ristova et al., 2013; Ristova and Busch, 2014; Slovak et al., 2014).

Extensive cellular measurements during leaf development have generated detailed insights into the cellular dynamics during the different phases of leaf growth. Obtaining these data is however laborious and/or time-consuming, arguing for more automated setups to obtain high-quality cell images suitable for data extraction. High-throughput imaging using spinning disc microscopy has recently been applied in plant research (Fitzgibbon et al., 2013) to perform large-scale imaging of the leaf epidermis.

Transcriptome analyses on different stages of leaf development (Beemster et al., 2005; Andriankaja et al., 2012) and on leaf growth mutants or transgenic lines have advanced our knowledge of leaf growth in the last years (Hepworth and Lenhard, 2014). However, within a growing leaf, different developmental cellular events occur and distinct cell layers with specialized functions are present. In monocot plant species, such as maize, these different growth zones are more straightforward to isolate, allowing high-resolution sampling of the leaves (Nelissen et al., 2012). Advanced sampling of developmental phase- and tissue-specific leaf material, facilitated by FACS (Gronlund et al., 2012; Adrian et al., 2015) or laser dissection isolation (Wuest and Grossniklaus, 2014) combined with RNA-sequencing, will result in cell- and stage-specific transcriptome maps that are already available for Arabidopsis roots (Birnbaum et al., 2003).

Mathematic modeling has been proven to be a great tool to better understand complex genetic networks (Middleton et al., 2010) and to predict patterning in Arabidopsis growth, such as phyllotaxis (Jönsson et al., 2006). Since leaf growth is a multifactorial trait, governed by multiple interconnected pathways, modeling will become increasingly important to further comprehend this complexity. Several models have been developed to describe cellular and leaf organ growth. The cell-based modeling framework VirtualLeaf allows users to investigate various aspects of tissue growth, such as cell division and growth, margin stiffness, tissue patterning and the interplay between them (https://code.google.com/p/virtualleaf/) (Merks et al., 2011). A mathematical model of the leaf epidermis, based on cellular dynamics of epidermal cells, has allowed measuring cell division and expansion rates during development and has showed that neighboring pavement cells with different sizes expanded at different relative rates (Kheibarshekan Asl et al., 2011). In addition, through time-lapse imaging of young leaves with confocal microscopy, growth dynamics and leaf shape formations were modeled, covering normal and perturbed growth of leaves (Kuchen et al., 2012). The creation of such models describing leaf growth will be facilitated with the availability of a multitude of data sets on rosette and individual leaf growth, cellular dynamics and the continuous elucidation of the molecular pathways that underlie leaf growth. Ideally, the outcome of single perturbations of the networks underlying leaf growth and the effect of multiple combinations would be predicted from these models in the future.

With recent advances in phenotyping techniques and platforms, RNA sequencing, and proteomic and metabolomic approaches, very large data sets on leaf growth are being produced in different labs world-wide. Ideally, these data sets can be integrated and used for meta-analysis to strengthen established findings and to identify new relationships between growth-regulating genes and mechanisms. This requires however an objective data description using coherent phenotype onthology and controlled vocabularies (Ilic et al., 2007; Avraham et al., 2008; Szakonyi et al., 2015) (http://www.plantontology.org/) and a correct description of the used phenotyping techniques. Similarly, a better annotation of the experimental metadata, such as a detailed description of environmental conditions, the timing and exact tissue of sampled material, must be provided to allow a correct comparison of data sets (Furbank and Tester, 2011; Fiorani and Schurr, 2013). For example, because growth of plants strongly differs between individual laboratories (Massonnet et al., 2010), the use of standardized descriptions of developmental stages, such as seedling stage 1.04, meaning the fourth rosette leaf becomes larger than 1 mm (Boyes et al., 2001), can provide more accurate information about the developmental timing than only reporting the amount of days after stratification of the seeds.

In plant growth, phenomics is an important research field, because it connects molecular changes with a visible phenotype. By further development of phenotyping methods and by combining phenomics with other research fields, such as genomics, metabolomics, proteomics and transcriptomics (Liberman et al., 2012), a complete and integrative systems biology view can be achieved, which will further extend our knowledge of leaf growth and development. In respect to this integrative view of leaf research, phenomics plays a central role since everything starts with the initial observation of a growth trait. A thorough phenotypic analysis can

in addition aid to select the most relevant timepoint and tissue to sample material for other -omics approaches. The underlying molecular mechanisms of the observations can be further tackled by, for example, exploring the transcriptomic and proteomic changes that underlie the growth phenotype. In addition, ionomics (Salt et al., 2008) combined with phenomics can provide valuable information about how mineral nutrients and spore elements are distributed in leaf tissue during its different developmental stages and how these elements are distributed under nutrient- and water-limiting conditions. Metabolic profiling of leaves during different developmental stages would deliver a better understanding of the sink-to-source transition in Arabidopsis and provide detailed insights into carbon allocation and nitrogen use under control and stress conditions. A similar sink-to-source profiling study has been successfully applied in the quaking aspen, which carries large leaves (Jeong et al., 2004), but this approach is very challenging using the small Arabidopsis leaves, because large amounts of material are required for metabolic profiling.

Outside the laboratory environment, a plethora of large-scale phenotyping methods is used in crop breeding and agriculture, and new approaches are developing in a rapid pace (Walter et al., 2015). For example, thermal remote sensing is used to estimate evaporation and drought stress agriculture (Maes and Steppe, 2012) and automatic phenotyping pipelines have been developed to monitor the color of grape berries in the field (Kicherer et al., 2015). In addition, the coverage of field monitoring can be increased by aerial phenotyping and multi-sensor approaches (Virlet et al., 2014; Liebisch et al., 2015).

Taken together, phenomics plays a central role in plant research as readout for underlying genetic or environmental changes. In addition, phenotyping helps to select the most appropriate timepoints and tissue for molecular characterization of the observed traits. Therefore, phenomics is an indispensable tool in the quest to understand leaf growth regulation.

ACKNOWLEDGEMENTS

We like to thank the Systems Biology of Yield group for the useful discussions and suggestions, Liesbeth De Milde, Marieke Dubois, Youn-Jeong Nam, Pieter Clauw, Federico Apelt, Nathalie Wuyts, Karen Lee, Rafael Abbeloos and Stefanie Polyn for providing images for the figures. We also thank Annick Bleys for her help in preparing this manuscript. This work was supported by grants from the Agency for Innovation by Science and Technology (IWT) for a predoctoral fellowship for H.V., the European Research Council under the European Union's Seventh Framework Programme (FP7/2007-2013; ERC grant agreement no. [339341-AMAIZE]11), Ghent University ("Bijzonder Onderzoeksfonds Methusalem project" no. BOF08/01M00408 and Multidisciplinary Research Partnership "Biotechnology for a Sustainable Economy" Grant 01MRB510W), and the Interuniversity Attraction Poles Program (IUAP P7/29 "MARS") initiated by the Belgian Science Policy Office.

REFERENCES

Adrian, J., et al. (2015). Transcriptome dynamics of the stomatal lineage: birth, amplification and termination of a self-renewing population. Dev. Cell **33:** 107-118.

Alvarez-Buylla, E.R., Benítez, M., Corvera-Poiré, A., Chaos Cador, Á., de Folter, S., Gamboa de Buen, A., Garay-Arroyo, A., García-Ponce, B., Jaimes-Miranda, F., Pérez-Ruiz, R.V., Piñeyro-Nelson, A., and Sánchez-Corrales, Y.E. (2010). Flower development. Arabidopsis Book **8:** e0127.

Andriankaja, M., Dhondt, S., De Bodt, S., Vanhaeren, H., Coppens, F., De Milde, L., Mühlenbock, P., Skirycz, A., Gonzalez, N., Beemster, G.T.S., and Inzé, D. (2012). Exit from proliferation during leaf development in *Arabidopsis thaliana*: a not-so-gradual process. Dev. Cell **22:** 64-78.

Apelt, F., Breuer, D., Nikoloski, Z., Stitt, M., and Kragler, F. (2015). Phytotyping^{4D}: a light-field imaging system for non-invasive and accurate monitoring of spatio-temporal plant growth. Plant J. **82:** 693-706.

Arvidsson, S., Pérez-Rodriguez, P., and Mueller-Roeber, B. (2011). A growth phenotyping pipeline for *Arabidopsis thaliana* integrating image analysis and rosette area modeling for robust quantification of genotype effects. New Phytol. **191:** 895-907.

Avraham, S., et al. (2008). The Plant Ontology Database: a community resource for plant structure and developmental stages controlled vocabulary and annotations. Nucleic Acids Res. **36:** D449-454.

Bayer, E.M., Smith, R.S., Mandel, T., Nakayama, N., Sauer, M., Prusinkiewicz, P., and Kuhlemeier, C. (2009). Integration of transport-based models for phyllotaxis and midvein formation. Genes Dev. **23:** 373-384.

Beeckman, T., and Viane, R. (2000). Embedding thin plant specimens for oriented sectioning. Biotech. Histochem. **75:** 23-26.

Beemster, G.T.S., De Veylder, L., Vercruysse, S., West, G., Rombaut, D., Van Hummelen, P., Galichet, A., Gruissem, W., Inzé, D., and Vuylsteke, M. (2005). Genome-wide analysis of gene expression profiles associated with cell cycle transitions in growing organs of Arabidopsis. Plant Physiol. **138:** 734-743.

Bensch, R., Ronneberger, O., Greese, B., Fleck, C., Wester, K., Hulskamp, M., and Burkhardt, H. (2009). Image analysis of Arabidopsis trichome patterning in 4D confocal datasets. In Biomedical Imaging: From Nano to Macro (Boston, Massachusetts, United states: IEEE), pp. 742-745.

Berger, S., Benediktyová, Z., Matouš, K., Bonfig, K., Mueller, M.J., Nedbal, L., and Roitsch, T. (2007). Visualization of dynamics of plant-pathogen interaction by novel combination of chlorophyll fluorescence imaging and statistical analysis: differential effects of virulent and avirulent strains of P-syringae and of oxylipins on A-thaliana. J. Exp. Bot. **58:** 797-806.

Bilgin, D.D., Zavala, J.A., Zhu, J., Clough, S.J., Ort, D.R., and DeLucia, E.H. (2010). Biotic stress globally downregulates photosynthesis genes. Plant Cell Environ. **33:** 1597-1613.

Birnbaum, K., Shasha, D.E., Wang, J.Y., Jung, J.W., Lambert, G.M., Galbraith, D.W., and Benfey, P.N. (2003). A gene expression map of the *Arabidopsis* root. Science **302:** 1956-1960.

Boyce, C.K. (2007). Mechanisms of laminar growth in morphologically convergent leaves and flower petals. Int. J. Plant Sci. **168:** 1151-1156.

Boyes, D.C., Zayed, A.M., Ascenzi, R., McCaskill, A.J., Hoffman, N.E., Davis, K.R., and Görlach, J. (2001). Growth stage-based phenotypic analysis of Arabidopsis: a model for high throughput functional genomics in plants. Plant Cell **13:** 1499-1510.

Candela, H., Martínez-Laborda, A., and Micol, J.L. (1999). Venation pattern formation in *Arabidopsis thaliana* vegetative leaves. Dev. Biol. **205:** 205-216.

Cao, J., et al. (2011). Whole-genome sequencing of multiple *Arabidopsis thaliana* populations. Nat. Genet. **43:** 956-963.

Chaerle, L., and Van Der Straeten, D. (2000). Imaging techniques and the early detection of plant stress. Trends Plant Sci. **5:** 495-501.

Chandler, J.W. (2012). Floral meristem initiation and emergence in plants. Cell. Mol. Life Sci. **69:** 3807-3818.

Cheng, P.-c., Lin, B.-L., Kao, F.-J., Gu, M., Xu, M.-G., Gan, X., Huang, M.-K., and Wang, Y.-S. (2001). Multi-photon fluorescence microscopy — the response of plant cells to high intensity illumination. Micron **32:** 661-669.

Cho, H.-T., and Cosgrove, D.J. (2000). Altered expression of expansin modulates leaf growth and pedicel abscission in *Arabidopsis thaliana*. Proc. Natl. Acad. Sci. USA **97:** 9783-9788.

Chou, H.-M., Bundock, N., Rolfe, S.A., and Scholes, J.D. (2000). Infection of *Arabidopsis thaliana* leaves with *Albugo candida* (white blister rust) causes a reprogramming of host metabolism. Mol. Plant Pathol. **1:** 99-113.

Christensen, S. (2010). Agarose imprints of plant cell surfaces for imaging. Cold Spring Harb. Protoc. **2010:** pdb.prot4932.

Cookson, S.J., Chenu, K., and Granier, C. (2007). Day length affects the dynamics of leaf expansion and cellular development in *Arabidopsis thaliana* partially through floral transition timing. Ann. Bot. **99:** 703-711.

Cosgrove, D.J. (2005). Growth of the plant cell wall. Nat. Rev. Mol. Cell Biol. **6:** 850-861.

De Veylder, L., Beeckman, T., Beemster, G.T.S., Krols, L., Terras, F., Landrieu, I., Van Der Schueren, E., Maes, S., Naudts, M., and Inzé, D. (2001). Functional analysis of cyclin-dependent kinase inhibitors of Arabidopsis. Plant Cell **13:** 1653-1667.

De Vylder, J., Vandenbussche, F., Hu, Y., Philips, W., and Van Der Straeten, D. (2012). Rosette Tracker: an open source image analysis tool for automatic quantification of genotype effects. Plant Physiol. **160:** 1149-1159.

Debernardi, J.M., Mecchia, M.A., Vercruyssen, L., Smaczniak, C., Kaufmann, K., Inzé, D., Rodriguez, R.E., and Palatnik, J.F. (2014). Post-transcriptional control of *GRF* transcription factors by microRNA miR396 and GIF co-activator affects leaf size and longevity. Plant J. **79:** 413-426.

Dhondt, S., Wuyts, N., and Inzé, D. (2013). Cell to whole-plant phenotyping: the best is yet to come. Trends Plant Sci. **18:** 428-439.

Dhondt, S., Vanhaeren, H., Van Loo, D., Cnudde, V., and Inzé, D. (2010). Plant structure visualization by high-resolution X-ray computed tomography. Trends Plant Sci. **15:** 419-422.

Dhondt, S., Van Haerenborgh, D., Van Cauwenbergh, C., Merks, R.M.H., Philips, W., Beemster, G.T.S., and Inzé, D. (2012). Quantitative analysis of venation patterns of Arabidopsis leaves by supervised image analysis. Plant J. **69:** 553-563.

Dhondt, S., Gonzalez, N., Blomme, J., De Milde, L., Van Daele, T., Van Akoleyen, D., Storme, V., Coppens, F., Beemster, G.T.S., and Inzé, D. (2014). High-resolution time-resolved imaging of *in vitro* Arabidopsis rosette growth. Plant J. **80:** 172-184.

Disch, S., Anastasiou, E., Sharma, V.K., Laux, T., Fletcher, J.C., and Lenhard, M. (2006). The E3 ubiquitin ligase BIG BROTHER controls *Arabidopsis* organ size in a dosage-dependent manner. Curr. Biol. **16:** 272-279.

Donnelly, P.M., Bonetta, D., Tsukaya, H., Dengler, R.E., and Dengler, N.G. (1999). Cell cycling and cell enlargement in developing leaves of *Arabidopsis*. Dev. Biol. **215:** 407-419.

Dornbusch, T., Michaud, O., Xenarios, I., and Fankhauser, C. (2014). Differentially phased leaf growth and movements in *Arabidopsis* depend on coordinated circadian and light regulation. Plant Cell **26:** 3911-3921.

Dornbusch, T., Lorrain, S., Kuznetsov, D., Fortier, A., Liechti, R., Xenarios, I., and Fankhauser, C. (2012). Measuring the diurnal pattern of leaf hyponasty and growth in *Arabidopsis* - a novel phenotyping approach using laser scanning. Funct. Plant Biol. **39:** 860-869.

El-Soda, M., Kruijer, W., Malosetti, M., Koornneef, M., and Aarts, M.G.M. (2014). Quantitative trait loci and candidate genes underlying genotype by environment interaction in the response of *Arabidopsis thaliana* to drought. Plant Cell Environ., in press (10.1111/pce.12418).

Eloy, N.B., et al. (2012). SAMBA, a plant-specific anaphase-promoting complex/cyclosome regulator is involved in early development and A-type cyclin stabilization. Proc. Natl. Acad. Sci. USA **109:** 13853-13858.

Elsner, J., Michalski, M., and Kwiatkowska, D. (2012). Spatiotemporal variation of leaf epidermal cell growth: a quantitative analysis of *Arabidopsis thaliana* wild-type and triple *cyclinD3* mutant plants. Ann. Bot. **109:** 897-910.

Ferjani, A., Horiguchi, G., Yano, S., and Tsukaya, H. (2007). Analysis of leaf development in *fugu* mutants of Arabidopsis reveals three compensation modes that modulate cell expansion in determinate organs. Plant Physiol. **144:** 988-999.

Fiorani, F., and Schurr, U. (2013). Future scenarios for plant phenotyping. Annu. Rev. Plant Biol. **64:** 267-291.

Fitzgibbon, J., Beck, M., Zhou, J., Faulkner, C., Robatzek, S., and Oparka, K. (2013). A developmental framework for complex plasmodesmata formation revealed by large-scale imaging of the *Arabidopsis* leaf epidermis. Plant Cell **25:** 57-70.

Forouzesh, E., Goel, A., Mackenzie, S.A., and Turner, J.A. (2013). *In vivo* extraction of Arabidopsis cell turgor pressure using nanoindentation in conjunction with finite element modeling. Plant J. **73:** 509-520.

Furbank, R.T., and Tester, M. (2011). Phenomics - technologies to relieve the phenotyping bottleneck. Trends Plant Sci. **16:** 635-644.

Gan, X., et al. (2011). Multiple reference genomes and transcriptomes for *Arabidopsis thaliana*. Nature **477:** 419-423.

Gandotra, N., Coughlan, S.J., and Nelson, T. (2013). The Arabidopsis leaf provascular cell transcriptome is enriched in genes with roles in vein patterning. Plant J. **74:** 48-58.

Geisler, M., Nadeau, J., and Sack, F.D. (2000). Oriented asymmetric divisions that generate the stomatal spacing pattern in Arabidopsis are disrupted by the *too many mouths* mutation. Plant Cell **12:** 2075-2086.

González-Bayón, R., Kinsman, E.A., Quesada, V., Vera, A., Robles, P., Ponce, M.R., Pyke, K.A., and Micol, J.L. (2006). Mutations in the *RETICULATA* gene dramatically alter internal architecture but have little effect on overall organ shape in *Arabidopsis* leaves. J. Exp. Bot. **57:** 3019-3031.

Gonzalez, N., Beemster, G.T.S., and Inzé, D. (2009). David and Goliath: what can the tiny weed *Arabidopsis* teach us to improve biomass production in crops? Curr. Opin. Plant Biol. **12:** 157-164.

Gonzalez, N., Vanhaeren, H., and Inzé, D. (2012). Leaf size control: complex coordination of cell division and expansion. Trends Plant Sci. **17:** 332-340.

Gonzalez, N., et al. (2010). Increased leaf size: different means to an end. Plant Physiol. **153:** 1261-1279.

Granier, C., and Vile, D. (2014). Phenotyping and beyond: modelling the relationships between traits. Curr. Opin. Plant Biol. **18:** 96-102.

Granier, C., et al. (2006). PHENOPSIS, an automated platform for reproducible phenotyping of plant responses to soil water deficit in *Arabidopsis thaliana* permitted the identification of an accession with low sensitivity to soil water deficit. New Phytol. **169:** 623-635.

Green, P.B., and Stanton, F.W. (1967). Turgor pressure: direct manometric measurement in single cells of Nitella. Science **155:** 1675-1676.

Gronlund, J.T., Eyres, A., Kumar, S., Buchanan-Wollaston, V., and Gifford, M.L. (2012). Cell specific analysis of Arabidopsis leaves using fluorescence activated cell sorting. Journal of visualized experiments : JoVE.

Guiboileau, A., Sormani, R., Meyer, C., and Masclaux-Daubresse, C. (2010). Senescence and death of plant organs: Nutrient recycling and developmental regulation. C. R. Biol. **333:** 382-391.

Harbinson, J., Prinzenberg, A.E., Kruijer, W., and Aarts, M.G.M. (2012). High throughput screening with chlorophyll fluorescence imaging and its use in crop improvement. Curr. Opin. Biotechnol. **23:** 221-226.

Hepworth, J., and Lenhard, M. (2014). Regulation of plant lateral-organ growth by modulating cell number and size. Curr. Opin. Plant Biol. **17:** 36-42.

Higa, S., Kobori, H., and Tsuchikawa, S. (2013). Mapping of leaf water content using near-infrared hyperspectral imaging. Appl. Spectrosc. **67:** 1302-1307.

Hoffmann, W.A., and Poorter, H. (2002). Avoiding bias in calculations of relative growth rate. Ann. Bot. **90:** 37-42.

Horiguchi, G., Kim, G.-T., and Tsukaya, H. (2005). The transcription factor AtGRF5 and the transcription coactivator AN3 regulate cell proliferation in leaf primordia of *Arabidopsis thaliana*. Plant J. **43:** 68-78.

Horiguchi, G., Fujikura, U., Ferjani, A., Ishikawa, N., and Tsukaya, H. (2006). Large-scale histological analysis of leaf mutants using two simple leaf observation methods: identification of novel genetic pathways governing the size and shape of leaves. Plant J. **48:** 638-644.

Horiguchi, G., Gonzalez, N., Beemster, G.T.S., Inzé, D., and Tsukaya, H. (2009). Impact of segmental chromosomal duplications on leaf size in the *grandifolia-D* mutants of *Arabidopsis thaliana*. Plant J. **60:** 122-133.

Hostettler, C., Kölling, K., Santelia, D., Streb, S., Kötting, O., and Zeeman, S.C. (2011). Analysis of starch metabolism in chloroplasts. Methods Mol. Biol. **775:** 387-410.

Hou, K., Wu, W., and Gan, S.-S. (2013). *SAUR36*, a SMALL AUXIN UP RNA gene, is involved in the promotion of leaf senescence in Arabidopsis. Plant Physiol. **161:** 1002-1009.

Huang, S., Raman, A.S., Ream, J.E., Fujiwara, H., Cerny, R.E., and Brown, S.M. (1998). Overexpression of 20-oxidase confers a gibberellin-overproduction phenotype in Arabidopsis. Plant Physiol. **118:** 773-781.

Ilic, K., et al. (2007). The plant structure ontology, a unified vocabulary of anatomy and morphology of a flowering plant. Plant Physiol. **143:** 587-599.

Inada, N., and Wildermuth, M.C. (2005). Novel tissue preparation method and cell-specific marker for laser microdissection of *Arabidopsis* mature leaf. Planta **221:** 9-16.

Jansen, M., et al. (2009). Simultaneous phenotyping of leaf growth and chlorophyll fluorescence via GROWSCREEN FLUORO allows detection of stress tolerance in *Arabidopsis thaliana* and other rosette plants. Funct. Plant Biol. **36:** 902-914.

Janssen, B.-J., and Gardner, R.C. (1989). Localized transient expression of GUS in leaf discs following cocultivation with *Agrobacterium*. Plant Mol. Biol. **14:** 61-72.

Janssens, O., De Vylder, J., Aelterman, J., Verstockt, S., Philips, W., Van Der Straeten, D., Van Hoecke, S., and Van de Walle, R. (2013). Leaf segmentation and parallel phenotyping for the analysis of gene networks in plants. In 2013 Proceedings of the 21st European Signal Processing Conference (EUSIPCO).

Jeong, M.L., Jiang, H., Chen, H.-S., Tsai, C.-J., and Harding, S.A. (2004). Metabolic profiling of the sink-to-source transition in developing leaves of quaking aspen. Plant Physiol. **136:** 3364-3375.

Jönsson, H., Heisler, M.G., Shapiro, B.E., Meyerowitz, E.M., and Mjolsness, E. (2006). An auxin-driven polarized transport model for phyllotaxis. Proc. Natl. Acad. Sci. USA **103:** 1633-1638.

Kalve, S., De Vos, D., and Beemster, G.T.S. (2014a). Leaf development: a cellular perspective. Front. Plant Sci. **5:** 362.

Kalve, S., Fotschki, J., Beeckman, T., Vissenberg, K., and Beemster, G.T.S. (2014b). Three-dimensional patterns of cell division and expansion throughout the development of *Arabidopsis thaliana* leaves. J. Exp. Bot. **65:** 6385-6397.

Kaminuma, E., Yoshizumi, T., Wada, T., Matsui, M., and Toyoda, T. (2008). Quantitative analysis of heterogeneous spatial distribution of Arabidopsis leaf trichomes using micro X-ray computed tomography. Plant J. **56:** 470-482.

Kawamura, E., Horiguchi, G., and Tsukaya, H. (2010). Mechanisms of leaf tooth formation in Arabidopsis. Plant J. **62:** 429-441.

Kazama, T., Ichihashi, Y., Murata, S., and Tsukaya, H. (2010). The mechanism of cell cycle arrest front progression explained by a *KLUH/CYP78A5*-dependent mobile growth factor in developing leaves of *Arabidopsis thaliana*. Plant Cell Physiol. **51:** 1046-1054.

Kerstetter, R.A., and Poethig, R.S. (1998). The specification of leaf identity during shoot development. Annu. Rev. Cell Dev. Biol. **14:** 373-398.

Khan, M., Rozhon, W., and Poppenberger, B. (2014). The role of hormones in the aging of plants - a mini-review. Gerontology **60:** 49-55.

Kheibarshekan Asl, L., Dhondt, S., Boudolf, V., Beemster, G.T.S., Beeckman, T., Inzé, D., Govaerts, W., and De Veylder, L. (2011). Model-based analysis of Arabidopsis leaf epidermal cells reveals distinct division and expansion patterns for pavement and guard cells. Plant Physiol. **156:** 2172-2183.

Kicherer, A., Herzog, K., Pflanz, M., Wieland, M., Rüger, P., Kecke, S., Kuhlmann, H., and Töpfer, R. (2015). An automated field phenotyping pipeline for application in grapevine research. Sensors **15:** 4823-4836.

Kölling, K., Müller, A., Flütsch, P., and Zeeman, S.C. (2013). A device for single leaf labelling with CO_2 isotopes to study carbon allocation and partitioning in *Arabidopsis thaliana*. Plant Methods **9:** 45.

Kölling, K., Thalmann, M., Müller, A., Jenny, C., and Zeeman, S.C. (2015). Carbon partitioning in *Arabidopsis thaliana* is a dynamic process controlled by the plants metabolic status and its circadian clock. Plant Cell Environ. **in press**.

Kong, W., Liu, F., Zhang, C., Bao, Y., Yu, J., and He, Y. (2014). Fast detection of peroxidase (POD) activity in tomato leaves which infected with *Botrytis cinerea* using hyperspectral imaging. Spectroc. Acta Pt. A-Molec. Biomolec. Spectr. **118:** 498-502.

Kuchen, E.E., Fox, S., Barbier de Reuille, P., Kennaway, R., Bensmihen, S., Avondo, J., Calder, G.M., Southam, P., Robinson, S., Bangham, A., and Coen, E. (2012). Generation of leaf shape through early patterns of growth and tissue polarity. Science **335:** 1092-1096.

Kuwabara, A., Backhaus, A., Malinowski, R., Bauch, M., Hunt, L., Nagata, T., Monk, N., Sanguinetti, G., and Fleming, A. (2011). A shift toward smaller cell size via manipulation of cell cycle gene expression acts to smoothen Arabidopsis leaf shape. Plant Physiol. **156:** 2196-2206.

Lee, B.H., Ko, J.-H., Lee, S., Lee, Y., Pak, J.-H., and Kim, J.H. (2009). The Arabidopsis *GRF-INTERACTING FACTOR* gene family performs an overlapping function in determining organ size as well as multiple developmental properties. Plant Physiol. **151:** 655-668.

Lee, K., Avondo, J., Morrison, H., Blot, L., Stark, M., Sharpe, J., Bangham, A., and Coen, E. (2006). Visualizing plant development and gene expression in three dimensions using optical projection tomography. Plant Cell **18:** 2145-2156.

Leister, D., Varotto, C., Pesaresi, P., Niwergall, A., and Salamini, F. (1999). Large-scale evaluation of plant growth in *Arabidopsis thaliana* by non-invasive image analysis. Plant Physiol. Biochem. **37:** 671-678.

Li, Y., Zheng, L., Corke, F., Smith, C., and Bevan, M.W. (2008). Control of final seed and organ size by the *DA1* gene family in *Arabidopsis thaliana*. Genes Dev. **22:** 1331-1336.

Liberman, L.M., Sozzani, R., and Benfey, P.N. (2012). Integrative systems biology: an attempt to describe a simple weed. Curr. Opin. Plant Biol. **15:** 162-167.

Liebisch, F., Kirchgessner, N., Schneider, D., Walter, A., and Hund, A. (2015). Remote, aerial phenotyping of maize traits with a mobile multi-sensor approach. Plant Methods **11:** 9.

Long, Q., et al. (2013). Massive genomic variation and strong selection in *Arabidopsis thaliana* lines from Sweden. Nat. Genet. **45:** 884-890.

Maes, W.H., and Steppe, K. (2012). Estimating evapotranspiration and drought stress with ground-based thermal remote sensing in agriculture: a review. J. Exp. Bot. **63:** 4671-4712.

Massonnet, C., et al. (2010). Probing the reproducibility of leaf growth and molecular phenotypes: a comparison of three Arabidopsis accessions cultivated in ten laboratories. Plant Physiol. **152:** 2142-2157.

Mathur, J., and Koncz, C. (1997). Method for preparation of epidermal imprints using agarose. Biotechniques **22:** 280-282.

Matouš, K., Benediktyová, Z., Berger, S., Roitsch, T., and Nedbal, L. (2006). Case study of combinatorial imaging: What protocol and what chlorophyll fluorescence image to use when visualizing infection of *Arabidopsis thaliana* by *Pseudomonas syringae*? Photosynth. Res. **90:** 243-253.

Matsuda, O., Tanaka, A., Fujita, T., and Iba, K. (2012). Hyperspectral imaging techniques for rapid identification of Arabidopsis mutants with altered leaf pigment status. Plant Cell Physiol. **53:** 1154-1170.

Mattsson, J., Sung, Z.R., and Berleth, T. (1999). Responses of plant vascular systems to auxin transport inhibition. Development **126:** 2979-2991.

McAusland, L., Davey, P.A., Kanwal, N., Baker, N.R., and Lawson, T. (2013). A novel system for spatial and temporal imaging of intrinsic plant water use efficiency. J. Exp. Bot. **64:** 4993-5007.

Melaragno, J.E., Mehrotra, B., and Coleman, A.W. (1993). Relationship between endopolyploidy and cell size in epidermal tissue of Arabidopsis. Plant Cell **5:** 1661-1668.

Merks, R.M.H., Guravage, M., Inzé, D., and Beemster, G.T.S. (2011). *VirtualLeaf*: an open source framework for cell-based modeling of plant tissue growth and development. Plant Physiol. **155:** 656-666.

Middleton, A.M., King, J.R., Bennett, M.J., and Owen, M.R. (2010). Mathematical modelling of the *Aux/IAA* negative feedback loop. Bull. Math. Biol. **72:** 1383-1407.

Mustroph, A., Zanetti, M.E., Jang, C.J.H., Holtan, H.E., Repetti, P.P., Galbraith, D.W., Girke, T., and Bailey-Serres, J. (2009). Profiling translatomes of discrete cell populations resolves altered cellular priorities during hypoxia in *Arabidopsis*. Proc. Natl. Acad. Sci. USA **106:** 18843-18848.

Mutz, K.-O., Heilkenbrinker, A., Lönne, M., Walter, J.-G., and Stahl, F. (2013). Transcriptome analysis using next-generation sequencing. Curr. Opin. Biotechnol. **24:** 22-30.

Nelissen, H., Rymen, B., Coppens, F., Dhondt, S., Fiorani, F., and Beemster, G.T.S. (2013). Kinematic analysis of cell division in leaves of mono- and dicotyledonous species: A basis for understanding growth and developing refined molecular sampling strategies. Methods Mol. Biol. **959:** 247-264.

Nelissen, H., Rymen, B., Jikumaru, Y., Demuynck, K., Van Lijsebettens, M., Kamiya, Y., Inzé, D., and Beemster, G.T.S. (2012). A local maximum in gibberellin levels regulates maize leaf growth by spatial control of cell division. Curr. Biol. **22:** 1183-1187.

Oh, S.A., Park, J.-H., Lee, G.I., Paek, K.H., Park, S.K., and Nam, H.G. (1997). Identification of three genetic loci controlling leaf senescence in *Arabidopsis thaliana*. Plant J. **12:** 527-535.

Ossowski, S., Schneeberger, K., Clark, R.M., Lanz, C., Warthmann, N., and Weigel, D. (2008). Sequencing of natural strains of *Arabidopsis thaliana* with short reads. Genome Res. **18:** 2024-2033.

Palatnik, J.F., Allen, E., Wu, X., Schommer, C., Schwab, R., Carrington, J.C., and Weigel, D. (2003). Control of leaf morphogenesis by microRNAs. Nature **425:** 257-263.

Pape, J.-M., and Klukas, C. (2014). 3-D histogram-based segmentation and leaf detection for rosette plants. Lecture Notes in Computer Science **8928:** 61-74.

Pérez-Pérez, J.M., Serrano-Cartagena, J., and Micol, J.L. (2002). Genetic analysis of natural variations in the architecture of *Arabidopsis thaliana* vegetative leaves. Genetics **162:** 893-915.

Pillitteri, L.J., and Dong, J. (2013). Stomatal development in Arabidopsis. Arabidopsis Book **11:** e0162.

Poethig, R.S. (2013). Vegetative phase change and shoot maturation in plants. Curr. Top. Dev. Biol. **105:** 125-152.

Poorter, H., Fiorani, F., Stitt, M., Schurr, U., Finck, A., Gibon, Y., Usadel, B., Munns, R., Atkin, O.K., Tardieu, F., and Ponsi, T.L. (2012). The art of growing plants for experimental purposes: a practical guide for the plant biologist. Funct. Plant Biol. **39:** 821-838.

Price, C.A., Symonova, O., Mileyko, Y., Hilley, T., and Weitz, J.S. (2011). Leaf extraction and analysis framework graphical user interface: segmenting and analyzing the structure of leaf veins and areoles. Plant Physiol. **155:** 236-245.

Redman, J.C., Haas, B.J., Tanimoto, G., and Town, C.D. (2004). Development and evaluation of an *Arabidopsis* whole genome Affymetrix probe array. Plant J. **38:** 545-561.

Ristova, D., and Busch, W. (2014). Natural variation of root traits: from development to nutrient uptake. Plant Physiol. **166:** 518-527.

Ristova, D., Rosas, U., Krouk, G., Ruffel, S., Birnbaum, K.D., and Coruzzi, G.M. (2013). RootScape: a landmark-based system for rapid screening of root architecture in Arabidopsis. Plant Physiol. **161:** 1086-1096.

Rodriguez, R.E., Debernardi, J.M., and Palatnik, J.F. (2014). Morphogenesis of simple leaves: regulation of leaf size and shape. Wiley Interdiscip. Rev.: Dev. Biol. **3:** 41-57.

Rolland-Lagan, A.-G., Amin, M., and Pakulska, M. (2009). Quantifying leaf venation patterns: two-dimensional maps. Plant J. **57:** 195-205.

Salt, D.E., Baxter, I., and Lahner, B. (2008). Ionomics and the study of the plant ionome. Annu. Rev. Plant Biol. **59:** 709-733.

Sawchuk, M.G., Head, P., Donner, T.J., and Scarpella, E. (2007). Time-lapse imaging of Arabidopsis leaf development shows dynamic patterns of procambium formation. New Phytol. **176:** 560-571.

Schmitz, R.J., Schultz, M.D., Urich, M.A., Nery, J.R., Pelizzola, M., Libiger, O., Alix, A., McCosh, R.B., Chen, H., Schork, N.J., and Ecker, J.R. (2013). Patterns of population epigenomic diversity. Nature **495:** 193-198.

Schneeberger, K., et al. (2011). Reference-guided assembly of four diverse *Arabidopsis thaliana* genomes. Proc. Natl. Acad. Sci. USA **108:** 10249-10254.

Skirycz, A., De Bodt, S., Obata, T., De Clercq, I., Claeys, H., De Rycke, R., Andriankaja, M., Van Aken, O., Van Breusegem, F., Fernie, A.R., and Inzé, D. (2010). Developmental stage specificity and the role of mitochondrial metabolism in the response of Arabidopsis leaves to prolonged mild osmotic stress. Plant Physiol. **152:** 226-244.

Skirycz, A., Claeys, H., De Bodt, S., Oikawa, A., Shinoda, S., Andriankaja, M., Maleux, K., Eloy, N.B., Coppens, F., Yoo, S.-D., Saito, K., and Inzé, D. (2011a). Pause-and-stop: the effects of osmotic stress on cell proliferation during early leaf development in *Arabidopsis* and a role for ethylene signaling in cell cycle arrest. Plant Cell **23:** 1876-1888.

Skirycz, A., et al. (2011b). Survival and growth of *Arabidopsis* plants given limited water are not equal. Nat. Biotechnol. **29:** 212-214.

Slovak, R., Göschl, C., Su, X., Shimotani, K., Shiina, T., and Busch, W. (2014). A scalable open-source pipeline for large-scale root phenotyping of *Arabidopsis*. Plant Cell **26:** 2390-2403.

Spartz, A.K., Lee, S.H., Wenger, J.P., Gonzalez, N., Itoh, H., Inzé, D., Peer, W.A., Murphy, A.S., Overvoorde, P.J., and Gray, W.M. (2012).

The *SAUR19* subfamily of *SMALL AUXIN UP RNA* genes promote cell expansion. Plant J. **70:** 978-990.

Streb, S., and Zeeman, S.C. (2012). Starch metabolism in Arabidopsis. Arabidopsis Book **10:** e0160.

Szakonyi, D., et al. (2015). The KnownLeaf literature curation system captures knowledge about *Arabidopsis* leaf growth and development and facilitates integrated data mining. Curr. Plant Biol. **2:** 1-11.

Tessmer, O.L., Jiao, Y., Cruz, J.A., Kramer, D.M., and Chen, J. (2013). Functional approach to high-throughput plant growth analysis. BMC Syst. Biol. **7:** S17.

Tisné, S., et al. (2013). Phenoscope: an automated large-scale phenotyping platform offering high spatial homogeneity. Plant J. **74:** 534-544.

Tsukaya, H. (2002). The leaf index: Heteroblasty, natural variation, and the genetic control of polar processes of leaf expansion. Plant Cell Physiol. **43:** 372-378.

Tsukaya, H. (2013a). Leaf development. Arabidopsis Book **11:** e0163.

Tsukaya, H. (2013b). Does ploidy level directly control cell size? Counterevidence from Arabidopsis genetics. PLoS ONE **8:** e83729.

Turner, S., and Sieburth, L.E. (2003). Vascular patterning. Arabidopsis Book **2:** e0073.

Ulmasov, T., Murfett, J., Hagen, G., and Guilfoyle, T.J. (1997). Aux/IAA proteins repress expression of reporter genes containing natural and highly active synthetic auxin response elements. Plant Cell **9:** 1963-1971.

Vanhaeren, H., Gonzalez, N., and Inzé, D. (2010). Hide and seek: uncloaking the vegetative shoot apex of *Arabidopsis thaliana*. Plant J. **63:** 541-548.

Vanhaeren, H., Gonzalez, N., Coppens, F., De Milde, L., Van Daele, T., Vermeersch, M., Eloy, N.B., Storme, V., and Inzé, D. (2014). Combining growth-promoting genes leads to positive epistasis in *Arabidopsis thaliana*. eLife **3:** e02252.

Vile, D., Pervent, M., Belluau, M., Vasseur, F., Bresson, J., Muller, B., Granier, C., and Simonneau, T. (2012). *Arabidopsis* growth under prolonged high temperature and water deficit: independent or interactive effects? Plant Cell Environ. **35:** 702-718.

Virlet, N., Lebourgeois, V., Martinez, S., Costes, E., Labbé, S., and Regnard, J.-L. (2014). Stress indicators based on airborne thermal imagery for field phenotyping a heterogeneous tree population for response to water constraints. J. Exp. Bot. **65:** 5429-5442.

Vlad, D., et al. (2014). Leaf shape evolution through duplication, regulatory diversification, and loss of a homeobox gene. Science **343:** 780-783.

Walter, A., Liebisch, F., and Hund, A. (2015). Plant phenotyping: from bean weighing to image analysis. Plant Methods **11:** 14.

Walter, A., Scharr, H., Gilmer, F., Zierer, R., Nagel, K.A., Ernst, M., Wiese, A., Virnich, O., Christ, M.M., Uhlig, B., Jünger, S., and Schurr, U. (2007). Dynamics of seedling growth acclimation towards altered light conditions can be quantified via GROWSCREEN: a setup and procedure designed for rapid optical phenotyping of different plant species. New Phytol. **174:** 447-455.

Wang, Z.-Y., Seto, H., Fujioka, S., Yoshida, S., and Chory, J. (2001). BRI1 is a critical component of a plasma-membrane receptor for plant steroids. Nature **410:** 380-383.

Weaver, L.M., and Amasino, R.M. (2001). Senescence is induced in individually darkened Arabidopsis leaves but inhibited in whole darkened plants. Plant Physiol. **127:** 876-886.

Weigel, D., and Mott, R. (2009). The 1001 Genomes Project for *Arabidopsis thaliana*. Genome Biol. **10:** 107.

White, D.W.R. (2006). *PEAPOD* regulates lamina size and curvature in *Arabidopsis*. Proc. Natl. Acad. Sci. USA **103:** 13238-13243.

Wilson-Sánchez, D., Rubio-Díaz, S., Muñoz-Viana, R., Pérez-Pérez, J.M., Jover-Gil, S., Ponce, M.R., and Micol, J.L. (2014). Leaf phenomics: a systematic reverse genetic screen for Arabidopsis leaf mutants. Plant J. **79:** 878-891.

Winter, D., Vinegar, B., Nahal, H., Ammar, R., Wilson, G.V., and Provart, N.J. (2007). An "electronic Fluorescent Pictograph" browser for exploring and analyzing large-scale biological data sets. PLoS ONE **2:** e718.

Wuest, S.E., and Grossniklaus, U. (2014). Laser-assisted microdissection applied to floral tissues. Methods Mol. Biol. **1110:** 329-344.

Wuyts, N., Massonnet, C., Dauzat, M., and Granier, C. (2012). Structural assessment of the impact of environmental constraints on *Arabidopsis thaliana* leaf growth: a 3D approach. Plant Cell Environ. **35:** 1631-1646.

Wuyts, N., Palauqui, J.-C., Conejero, G., Verdeil, J.-L., Granier, C., and Massonnet, C. (2010). High-contrast three-dimensional imaging of the Arabidopsis leaf enables the analysis of cell dimensions in the epidermis and mesophyll. Plant Methods **6:** 17.

Yu, K.-Q., Zhao, Y.-R., Li, X.-L., Shao, Y.-N., Liu, F., and He, Y. (2014). Hyperspectral imaging for mapping of total nitrogen spatial distribution in pepper plant. PLoS ONE **9:** e116205.

Zhang, X., Hause Jr., R.J., and Borevitz, J.O. (2012). Natural genetic variation for growth and development revealed by high-throughput phenotyping in *Arabidopsis thaliana*. G3: Genes, Genomes, Genet. **2:** 29-34.